Journal of Energy Storage 75 (2024) 109671

Contents lists available at ScienceDirect

Journal of Energy Storage

journal homepage: www.elsevier.com/locate/est

Research papers

FC-PV-battery-Z source-BBO integrated unified power quality conditioner for sensitive load & EV charging station

Krishna Sarker *

Department of Electrical Engineering, St. Thomas' College of Engineering & Technology, West Bengal, India

ARTICLE INFO

Keywords:
FC-PV-Battery-Z source-BBO based Unified Power Quality Conditioner (UPQC)
Biogeography-Based Optimization (BBO)-based Selected Harmonic Elimination
FC-PV-Battery-Z source-BBO based STATCOM (Static Synchronous Compensator)
FC-PV-Battery-Z source-BBO based Dynamic Voltage Restorer
Enhance Power Quality (PQ)
Improvement of EV Charging Station with Dual Active Bridge (DAB)

ABSTRACT

The proposed integrated system combines of fuel cell (FC), photovoltaic (PV), battery, Z-source and Biogeography-Based Optimization (BBO) based Unified Power Quality Conditioner (UPQC) compensator aims to provide a high-quality power supply to sensitive loads, such as electrical, electronics, medical equipment, Electrical Vehicles (EV), or critical industrial processes. It can regulate voltage, mitigate power disturbances (e.g., voltage sags, swells, flicker, voltage interruption, harmonics, reactive power etc.), and ensure a stable power supply. Additionally, it can facilitate EV charging stations by managing the power flow and optimizing charging processes. The PV or FC based Z-source inverter can control and regulate power flow in both directions. It operates with a unique impedance network, allowing for voltage boosting or bucking. The Z-source inverter enhances the flexibility and control of power flow in the system. The fuel cell generates electricity through an electrochemical process, typically using hydrogen as a fuel source, while the PV array converts sunlight into electrical energy. The FC-PV system provides a renewable and clean energy source. The battery serves as an energy storage device within the integrated UPQC system. It stores excess energy produced by the FC-PV system or from the grid during off-peak hours and releases it when needed, contributing to load balancing and stability. Biogeography-Based Optimization (BBO)-based Selected Harmonic Elimination Pulse Width Modulation (SHE-PWM) technique calculate the proper inverter switching angles and control the total harmonic distortion (% THD). Grid connected EV charging station produce nonlinear current and pollute the DC-link system. The proposed FC-PV-Z source-BBO based UPQC and its control strategy can enhance the EV-charging induced PQ (power quality) issues, eliminate the voltage and current harmonic or reduce overall voltage and current %THD control the proper reactive power, improve the power factor, restoring the flicker, transient, swells and sags of the micro grid, grid or smart grid and completely moderate the fluctuations of DC-link voltage.

1. Introduction

A Unified Power Quality Conditioner (UPQC) is a power electronic switching device used to mitigate the any type of power quality issues in electrical grid, micro-grid and smart grid systems. Proposed Fuel cell-PV-battery based UPQC model is a smarter system. It combines functionalities of both a shunt active power filter (SAPF) and a series active power filter (SAPF) in a single unit. A UPQC [1–10] can compensate for voltage sags [1], voltage swells [1,2], voltage harmonics [3], flicker [4], and reactive power [5], among other power quality [6–10] problems.

A UPQC can be integrated with different renewable energy sources [11] for enhanced power quality and stability. In this literature [11], author delve into the exploration of how Unified Power Quality Conditioner (UPQC) can effectively address power quality issues within the grid and combat harmonics introduced by non-linear loads. The study specifically incorporates the assistance of Photovoltaic (PV) and Battery Energy Storage System (BESS). In this setup, the PV system plays a pivotal role in supplying active power to the load. One possible combination is integrating a fuel cell [12], photovoltaic (PV) [13] and battery [14] system with a UPQC. Here's how this integration can work:

1. Fuel Cell [12]: The fuel cell provides a constant and reliable source of electrical power. It converts the chemical energy of a fuel, such as hydrogen, into electricity through an electrochemical process. The fuel cell system can supply power to the UPQC and other loads, contributing to overall power quality improvement.
2. PV System [13]: The PV system harnesses solar energy and converts it into electricity. It consists of photovoltaic modules that generate

* Corresponding author.
E-mail address: krishna80sarker@gmail.com.

https://doi.org/10.1016/j.est.2023.109671
Received 30 June 2023; Received in revised form 24 October 2023; Accepted 9 November 2023
Available online 16 November 2023

DC power when exposed to sunlight. This DC power is then converted into AC power through an inverter. The PV system can also provide power to the UPQC and other loads, complementing the fuel cell's power generation.

3. UPQC Integration [14,15]: The UPQC is connected in parallel with the load and the distribution system. It consists of a shunt active power filter (SAPF) connected in parallel with the load and a series active power filter (SAPF) connected in series with the distribution system. The SAPF compensates for load-generated harmonics and reactive power, while the SAPF mitigates voltage disturbances and regulates voltage levels.

By integrating a fuel cell, battery and PV system with a UPQC, several benefits can be achieved:

i. Power Quality Improvement: The UPQC can correct voltage sags, swells, and harmonics caused by load variations, grid disturbances, or renewable energy source fluctuations. It ensures a stable and high-quality power supply to sensitive loads.
ii. Enhanced Renewable Energy Integration: The combination of a fuel cell and PV system with a UPQC allows for efficient and reliable integration of renewable energy sources into the electrical grid. The UPQC ensures that the power injected into the grid meets the required quality standards.
iii. Grid Support: The UPQC can provide reactive power compensation and voltage regulation, which helps maintain grid stability and reduces power losses.
iv. Energy Efficiency: By compensating for reactive power and harmonics, the UPQC improves the overall power factor and reduces energy losses, contributing to increased energy efficiency.
v. Z-source inverter [16] is a type of power inverter that has a unique impedance network that allows it to buck and boost the input voltage. It differs from traditional inverters in that it uses an impedance network instead of a DC link capacitor to couple the inverter circuit to the source. This makes it more efficient and reliable than traditional inverters.
vi. In a Z-source inverter [16], the impedance network is connected between the DC source and the inverter circuit. The network consists of two inductors and two capacitors that are connected in a unique configuration. The inductors are connected in series with the DC source, while the capacitors are connected in parallel with the inverter circuit. This configuration allows the inverter to buck and boost the input voltage by controlling the shoot-through state of the switches. The shoot-through state is when both switches are turned on at the same time, which creates a short circuit across the DC source. This short circuit causes the voltage across the inductors to increase, which boosts the output voltage of the inverter. Conversely, when one switch is turned off and the other is turned on, the voltage across the inductors decreases, which causes the output voltage of the inverter to decrease as well. This makes it possible for Z-source inverters to operate with a wider range of input voltages than traditional inverters.
vii. Z-source inverters are used in a variety of applications, including renewable energy systems, electric vehicles, and motor drives. They are particularly useful in applications that require a wide range of input voltages or that have limited DC voltage sources.
viii. Power quality [1–18] refers to the reliability and stability of the electrical power supply. It encompasses various aspects, including voltage stability, frequency variation, harmonics, and interruptions. Ensuring good power quality is crucial for the efficient and safe operation of electrical systems and the optimal performance of connected devices. Power quality issues, such as voltage sags, surges, and harmonic distortions, can lead to equipment malfunction, increased energy consumption, and even damage to electrical components. Mitigating power quality challenges often involves the use of technologies like power conditioners, voltage regulators, and filters to maintain a stable and high-quality power supply.

The article [19] introduces a pioneering concept of the three-phase multi-objective unified power quality conditioner (MO-UPQC). This innovative apparatus incorporates interfaces tailored for solar photovoltaic (PV) panels and energy storage in batteries. The MO-UPQC exhibits the capacity to rectify power quality issues in both voltages (at the load side) and currents (at the power grid side). The results garnered from these [19] experiments underscore the feasibility and broad applicability of the MO-UPQC, affirming its potential as a versatile solution in addressing diverse power quality challenges and showcasing its adaptability across a spectrum of scenarios. The literature [20] introduces a standalone three-phase system designed for enhancing power quality (PQ) on both the load side voltages and the currents at the machine terminal. The central component of this autonomous system is a three-phase permanent magnet synchronous generator (PMSG) propelled by a governor-less hydro turbine, serving as the three-phase source to power sensitive, nonlinear, and linear loads. Connectivity is established through a unified power quality conditioner (UPQC). The UPQC's shunt compensator plays a pivotal role in addressing current quality concerns, encompassing reactive power compensation and harmonics elimination. This dual functionality enables the system to concurrently enhance voltage quality issues.

In [21], this literature review, we delve into the introduction of an advanced control methodology utilizing an Enhanced Second-Order Generalized Integrator (ESOGI) for a grid-integrated Unified Power Quality Conditioner (UPQC) incorporating a solar photovoltaic (PV) system. The primary aim of this [21] approach is to elevate power quality (PQ) indices within the grid, achieved through the elimination of voltage sensors on the grid side in the comprehensive control framework. Furthermore, the presented control method demonstrates a high degree of efficacy in eliminating the DC component, contributing to enhanced power quality in the integrated system. The acritical [22] not only enhances the efficiency of the distribution system but also contributes to cost reduction, ensures a continuous power supply, and diminishes the need for frequent maintenance. To combat issues such as voltage sags, swells, transients, imbalances, and current harmonics in distribution systems, UPQC custom power devices have been introduced. Among these [22], the Unified Power Quality Conditioner (UPQC) stands out as a frequently employed solution, playing a pivotal role in elevating the overall power quality of distribution systems. In the realm of literature [23], it has been observed that electric vehicle charging stations connected to distribution grids introduce nonlinear current, leading to power quality concerns such as harmonic distortion and DC-link fluctuation. Recent studies [23] highlight the efficacy of a Unified Power Quality Conditioner with Superconducting Magnetic Energy Storage (UPQC-SMES) in mitigating the power quality issues arising from electric vehicle charging, offering a promising solution to address these challenges. Within [24] study, a Hybrid Active Power Filter with Photovoltaic (HAPF-PV) is explored, employing a combination of a second-order sequence filter (SOSF) and a proportional–integral (PI) controller for power quality improvement.

In this literature [25] review, the focus is on a distributed generation (DG) system that integrates a photovoltaic (PV) system with a 1-Phase to 3-Phase Unified Power Quality Conditioner (UPQC-1PH-3PH). Referred to as DG-UPQC-1PH-3PH, this system plays a dual role by injecting energy produced from a PV array into the grid and supplying loads connected to a local three-phase four-wire electrical system. It serves the needs of consumers in rural or remote areas supplied by a single-phase utility. Beyond the injection of active power, DG-UPQC-1PH-3PH significantly enhances power quality indicators, addressing issues such as voltage sags/swells, grid voltage harmonics, and power factor. Exploring the Interplay of FACTS Devices and Electric Vehicles in Distribution Networks: An In-depth Technological Review on Challenges and Opportunities in the article [26]. In paper [27], Optimizing Multi-

Converter Unified Power Quality Conditioner for Enhanced Power Quality: A Literature Review Employing the Beetle Swarm-Based Butterfly Optimization Algorithm.

In addressing power quality concerns related to SHE, conventional approaches take the lead. However, these approaches have drawbacks, including a tendency to get stuck in locally optimal solutions and a reliance on specific initial parameters. A solution to overcome these challenges is the adoption of metaheuristic algorithms. In this research, author initially employed 12 metaheuristic algorithms, each drawing inspiration from diverse sources, to address the SHE problem across various modulation indices in both 180-degree and 120-degree conduction modes. Subsequently, author conducted a comprehensive analysis of their performances.

While the mentioned methods offer swift and efficient solutions, they grapple with issues like local optima, sluggish convergence, and the need for intricate multi-parameter tuning. Additionally, the validation of an algorithm's superiority over others is hindered by a lack of comprehensive case studies. The performance of these algorithms exhibits considerable variation, contingent on parameters like the inverter's produced voltage levels, targeted harmonics, switching angles, and sets of nonlinear equations within the Sinusoidal Pulse Width Modulation (SHEPWM) framework. Consequently, there arises a demand for an algorithm that can demonstrate its superiority across diverse case studies, accommodating different sets of parameters.

The existing research on inverter switching angle calculation and harmonic elimination has extensively explored various optimization algorithms such as Firefly Algorithm (FA) [28], Teaching-Learning-Based Optimization (TLBO) [29], Particle Swarm Optimization (PSO) [30], Gravitational Search Algorithm (GSA) [31,32], Cuckoo Search Algorithm (CSA) [33], Genetic Algorithms (GA) [34], Red Deer Algorithm (RDA) [35], Biogeography-based Optimization (BBO) [17], Artificial Neural Networks (ANN) [36], Grey Wolf Optimizer (GWO) [37], Bat Algorithm (BA) [38,39] and Soccer League Optimization (SLO) [3] method. However, there is a noticeable research gap in understanding the comparative effectiveness and efficiency of these algorithms specifically in the context of minimizing selected harmonics during inverter switching angle calculation. The literature lacks a comprehensive analysis that identifies the strengths and weaknesses of each optimization method concerning harmonic elimination, hindering the development of guidelines for selecting the most suitable algorithm for this particular application. Addressing this gap could significantly contribute to the optimization of inverter performance in power grid, providing valuable insights for researchers and practitioners in the field. In all the above-mentioned studies, it has been shown that the proposed Biogeography-based Optimization (BBO) algorithms is the most suitable and it can effectively remove unwanted harmonics, improve the power quality by the control strategy.

The integration of a fuel cell, battery, PV system, and UPQC offers a comprehensive solution for power quality enhancement, renewable energy integration, and grid support. It combines the benefits of clean energy generation with advanced power conditioning capabilities, leading to a more sustainable and reliable electrical system. Our proposed model mitigates all the power quality issues with harmonic problems for minimum switching scheme. To identify the switching angles that are best for the SHEAM-PWM technique with elimination or reduction of the greatest number of harmonics from the output voltage waveform, the BBO approach is taken into account. Angles are computed offline to remove lower order harmonics and suppressed higher order harmonics, and utilizing mixed model equations, they are then saved in microcontroller memory for online use.

2. Proposed FC-PV-Battery-Z source based Unified Power Quality Conditioner (UPQC) with EV charging

Fig. 1 illustrates the proposed model featuring a FC-PV-Battery-Z source-based Unified Power Quality Conditioner (UPQC) alongside an EV Charger equipped with a Dual Active Bridge. A Unified Power Quality Conditioner (UPQC) is a power electronic device that combines the functionalities of a Static Synchronous Compensator (STATCOM) and a Static Voltage Regulator (SVR) into a single unit. It is used for comprehensive power quality improvement in electrical power systems. The UPQC is designed to mitigate various power quality issues, including voltage sags, swells, interruptions, harmonics, and reactive power fluctuations. It can simultaneously regulate the voltage at the point of common coupling (PCC) and compensate for current-related disturbances, making it an effective solution for power quality enhancement. A two-stage power conversion with high-frequency (HF) isolation is present in the EV charger. It consists of a three-phase VSC for active rectification and a three-level dual active bridge (DAB) dc-dc converter to control battery charging rate. Through interface boost inductors, the VSC is connected to the three-phase grid on one side and to the dc-link capacitor on the other.

The UPQC consists of two main components:

A. **Shunt Active Power Filter (SAPF):** The SAPF is connected in parallel with the load and acts as a STATCOM. It compensates for

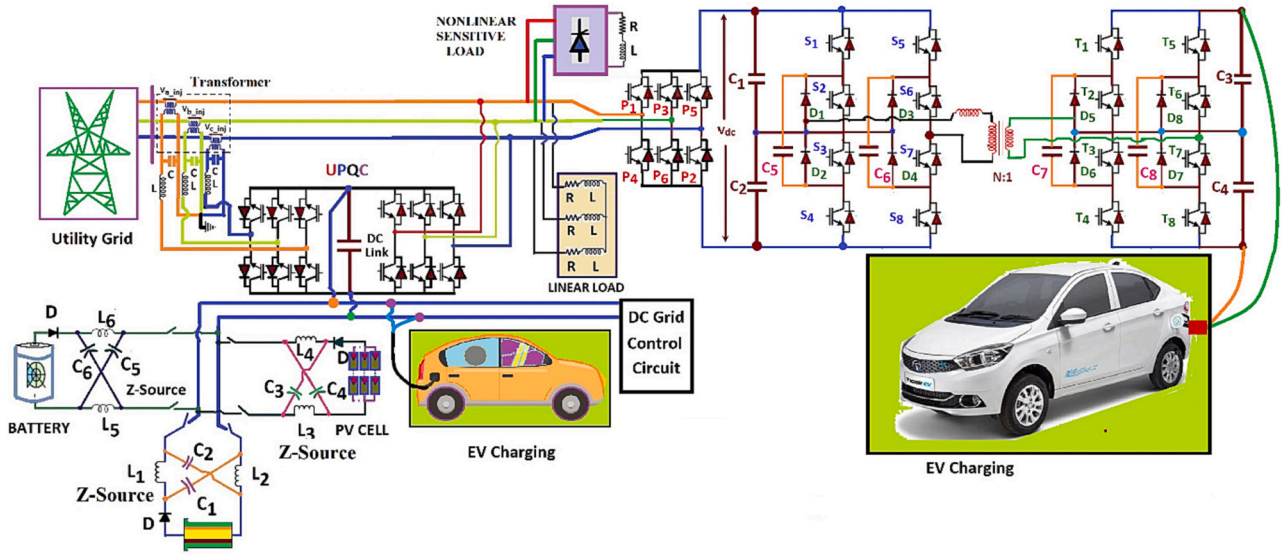

Fig. 1. Proposed model of FC-PV-Battery-Z source based UPQC and EV charger with dual active bridge.

reactive power, controls voltage fluctuations, and mitigates harmonic distortions. The SAPF uses voltage source converter (VSC) technology to inject or absorb reactive power as required and maintain the load voltage within the desired limits.

The power electronic switching device STATCOM is used for reactive power compensation and voltage regulation in electrical power systems. It belongs to the family of Flexible AC Transmission Systems (FACTS) devices and is based on Voltage Source Converter (VSC) technology.

The primary function of a STATCOM is to regulate the voltage at a specific point in the electrical network by injecting or absorbing reactive power as needed. It helps to maintain a stable voltage profile, improve power quality, and enhance the overall performance of the power system. The STATCOM is typically connected in parallel to the network and can quickly respond to changes in load conditions or system disturbances.

The key components of a STATCOM include a VSC, a DC capacitor bank or energy storage device, and a control system. The VSC consists of insulated-gate bipolar transistors (IGBTs) or other power semiconductor devices that can switch rapidly to control the flow of reactive power. The DC capacitor bank provides the necessary energy storage to support the reactive power exchange.

The control system of a STATCOM continuously monitors the voltage and reactive power at the point of connection and adjusts the output of the VSC accordingly. When the voltage deviates from the desired setpoint, the STATCOM injects or absorbs reactive power to regulate the voltage. The control system uses advanced algorithms and feedback loops to maintain voltage stability and respond to dynamic changes in the system.

Benefits of STATCOM for proposed model include:

a. **Voltage regulation:** STATCOMs can help maintain voltage levels within the desired range, even during fluctuating loads or disturbances in the grid.
b. **Reactive power compensation:** STATCOMs can inject or absorb reactive power to improve power factor and reduce system losses.
c. **Fast response time:** STATCOMs can respond to voltage fluctuations within a few milliseconds, providing rapid and accurate voltage support.
d. **Dynamic voltage stability:** STATCOMs enhance the stability and reliability of the power system by damping voltage oscillations and controlling voltage rise/fall rates.
e. **Harmonic mitigation:** STATCOMs can reduce harmonics in the system by actively filtering out unwanted harmonic components.

STATCOMs find applications in various scenarios, including distribution networks, transmission systems, renewable energy integration, industrial plants, and large-scale commercial facilities. They play a crucial role in maintaining grid stability, enabling increased power transfer capability, and improving power quality.

B. **Series Voltage Compensator (SVC) or Dynamic Voltage Restorer DVR for proposed model:** The SVC is connected in series with the supply line and operates as an SVR or custom power DVR. It regulates the voltage magnitude and compensates for voltage sags, swells, and interruptions. The SVC/DVR injects or absorbs active power to maintain a stable voltage at the PCC and protect sensitive loads from disturbances.

Both components of the UPQC are controlled by a common control system that continuously monitors the voltage and current at the PCC. Based on the detected disturbances, the control system dynamically adjusts the output of the SAPF and SVC to provide real-time compensation. The control algorithms for the UPQC are designed to optimize performance and ensure seamless coordination between the shunt and series compensators.

A Dynamic Voltage Restorer (DVR) is used to mitigate voltage sags and swells in electrical power systems. Voltage sags and swells can occur due to various reasons such as faults, sudden changes in load, or switching operations. These disturbances can have detrimental effects on sensitive equipment and can lead to disruptions in industrial processes or damage to electrical appliances.

The DVR is designed to inject a compensating voltage into the power system to regulate the voltage at the point of common coupling (PCC), which is typically the interface between the utility grid and the customer's electrical system. By monitoring the voltage at the PCC and rapidly injecting or absorbing reactive power, the DVR can maintain a stable and regulated voltage profile, regardless of disturbances in the grid.

The main components of a DVR typically include a power converter, energy storage device (such as batteries or capacitors), and control circuitry. When a voltage sag or swell is detected, the DVR rapidly switches its power converter to inject or absorb the necessary reactive power to compensate for the disturbance. The energy storage device provides the necessary energy to support the compensation during the transient period.

The proposed DVRs offer several advantages in power quality improvement, including:

I. **Voltage stabilization:** DVRs can quickly respond to voltage disturbances and restore the voltage to its nominal level, minimizing the impact on sensitive loads.
II. **Fast response time:** DVRs have high-speed control systems that enable them to detect and respond to voltage sags or swells within a few milliseconds.
III. **Flexibility:** DVRs can be installed at specific points in the distribution system to provide targeted voltage regulation where it is needed most.
IV. **Compatibility:** DVRs can be integrated with various types of electrical systems and do not require major modifications to the existing infrastructure.
V. **Cost-effectiveness:** DVRs can be a cost-effective solution compared to other alternatives such as uninterruptible power supplies (UPS) or voltage regulators.

DVRs have found applications in a wide range of industries, including manufacturing, data centers, hospitals, and critical infrastructure facilities. They help ensure a reliable power supply, reduce downtime, and protect sensitive equipment from voltage disturbances.

Advantages of Proposed FC-battery-PV based UPQC include:

- **Comprehensive power quality improvement:** UPQC can simultaneously address multiple power quality issues, including voltage regulation, reactive power compensation, harmonic mitigation, and load balancing.
- **Enhanced voltage stability:** UPQC can maintain stable voltage levels even under varying load conditions and grid disturbances, thereby reducing the risk of equipment damage and downtime.
- **Increased power transfer capability:** By compensating for reactive power and voltage fluctuations, UPQC enables increased power transmission capacity in the grid.
- **Compatibility and flexibility:** UPQC can be integrated into existing power systems without requiring major modifications, making it a versatile solution for both distribution and transmission networks.
- **Cost-effective solution:** UPQC eliminates the need for separate devices for voltage regulation and reactive power compensation, resulting in reduced capital and maintenance costs.

UPQC finds applications in a wide range of industries, including manufacturing plants, data centers, renewable energy systems, and sensitive facilities where power quality is critical. It helps improve system reliability, reduce energy losses, and enhance the overall power quality for both utilities and end-users.

2.1. Function of Z-source based inverter for proposed UPQC

A Z-source inverter (ZSI) is a type of power electronic converter used in electrical systems to convert DC (direct current) power to AC (alternating current) power. It is an alternative to traditional inverters, such as the voltage-source inverter (VSI) and current-source inverter (CSI), and offers certain advantages in terms of input voltage range and boosting capabilities.

The ZSI gets its name from the unique impedance network, known as the "Z-network," which is incorporated into its design. The Z-network consists of two power components connected in series, forming a "shoot-through" path. These components are typically inductive and capacitive elements, such as inductors and capacitors.

The key advantage of the ZSI is its ability to provide both voltage buck and boost capabilities. In traditional inverters, the input voltage must be higher than the output voltage for boosting operations. However, the ZSI can handle voltage boosting even when the input voltage is lower than the output voltage. This is achieved by controlling the shoot-through state of the Z-network.

The shoot-through state occurs when both power components in the Z-network are simultaneously conducting. During this state, the input voltage is temporarily connected directly to the output, allowing energy to flow from the input to the output without being limited by the input voltage level. By controlling the shoot-through state, the ZSI can regulate the output voltage and achieve voltage boosting.

The ZSI has applications in various fields, including renewable energy systems, electric vehicles, and motor drives. It offers advantages such as improved efficiency, reduced size and weight, and enhanced reliability. However, it also poses challenges in terms of control complexity and increased semiconductor stress due to shoot-through operation. In summary, a Z-source inverter is that utilizes a unique impedance network to provide voltage buck and boost capabilities. It offers advantages over traditional inverters in certain applications and is an area of ongoing research and development in the field of power electronics.

2.2. Function of fuel cell (FC) for proposed UPQC

A fuel cell is an electrochemical device that converts the chemical energy of a fuel, typically hydrogen, directly into electrical energy without combustion. It operates based on the principles of redox reactions, utilizing an electrolyte to facilitate the conversion process.

Here's a simplified overview of how a fuel cell works in proposed UPQC Model:

A. **Fuel Input:** The fuel cell requires a fuel source, commonly hydrogen gas (H_2), although other fuels such as methanol can also be used. The fuel is supplied to the anode (negative electrode) of the fuel cell.
B. **Electrolyte:** The fuel cell consists of an electrolyte, which can be a solid, liquid, or polymer membrane. The most common types of fuel cells include proton exchange membrane fuel cells (PEMFCs), solid oxide fuel cells (SOFCs), and molten carbonate fuel cells (MCFCs). The electrolyte facilitates the movement of ions between the anode and the cathode.
C. **Electrochemical Reaction:** At the anode, the fuel undergoes a catalytic reaction (typically facilitated by a platinum-based catalyst) that splits the hydrogen molecules into protons (H^+) and electrons (e^-). The protons pass through the electrolyte, while the electrons travel through an external circuit, creating an electrical current.
D. **Oxygen Input:** At the cathode (positive electrode), oxygen (O_2) from the air or an external source is supplied. In PEMFCs, the cathode also contains a catalyst to facilitate the oxygen reduction reaction.
E. **Electrochemical Reaction (continued):** At the cathode, the protons from the anode combine with the oxygen and electrons to form water (H_2O). This reaction releases energy in the form of heat.
F. **Electrical Output:** The flow of electrons through the external circuit generates electrical power that can be utilized to power electrical devices or charge batteries.

Fuel cells offer several advantages for Proposed UPQC:

a) **Efficiency:** Fuel cells have higher efficiency compared to traditional combustion-based systems, as they convert chemical energy directly into electrical energy, bypassing the intermediate thermal conversion.
b) **Clean and Environmentally Friendly:** Hydrogen fuel cells produce only water and heat as byproducts, making them environmentally friendly and free from harmful emissions.
c) **Quiet Operation:** Fuel cells operate silently compared to internal combustion engines.
d) **Versatility:** Fuel cells can be scaled up or down to meet various power requirements, from small portable devices to large-scale power generation.

However, there are challenges associated with fuel cells:

(1) **Hydrogen Infrastructure:** The availability and infrastructure for producing, storing, and distributing hydrogen fuel is limited, which poses a challenge for widespread adoption.
(2) **Cost:** The cost of fuel cells, especially those utilizing expensive catalyst materials like platinum, remains relatively high compared to conventional energy sources.
(3) **Durability and Lifetime:** Ensuring the long-term durability and lifetime of fuel cells, especially in harsh operating conditions, is an ongoing area of research and development.

Despite these challenges, fuel cells hold promise for various applications for power quality problems, stationary power generation, and portable electronics, offering a cleaner and more sustainable energy alternative.

UPQC stands for "Unified Power Quality Conditioner". It is a power electronics-based device that is used to improve the quality of power supplied to sensitive loads. A Z-source, Fuel cell and PV based UPQC is a device that uses both fuel cells and photovoltaic cells to improve the quality of power supplied to sensitive loads.

The fuel cell generates electricity by converting the chemical energy of hydrogen and oxygen into electrical energy. The photovoltaic cells generate electricity by converting sunlight into electrical energy. The UPQC then uses this electricity to improve the quality of power supplied to sensitive loads by regulating voltage and current. For more advantageous the Z-source, Fuel cell and PV based UPQC can be used in various applications such as electric vehicles, renewable energy systems, and distributed generation systems. They can also be used in industries such as aerospace, telecommunications, and healthcare.

3. Proposed harmonic elimination technique

The Biogeography-Based Optimization (BBO) algorithm is a metaheuristic optimization technique inspired by the principles of biogeography, which is the study of the geographical distribution of biological organisms. BBO mimics the process of migration and species distribution to solve the inverter optimum switching angles for nonlinear optimization problems.

The proposed method (BBO-based Selected Harmonic Elimination Pulse Width Modulation technique) determines optimum switching angles for inverters in an off-line mode. These switching angles are calculated to eliminate lower order harmonics. The obtained optimal switching angles are then stored in the microcontroller processor's memory using mixed model equations (MME).

During online application, the microcontroller retrieves the stored switching angles from memory and uses them to control the inverter in

real-time. By employing the BBO-based SHE-PWM technique [17,18], the goal is to achieve harmonic elimination and improve the power quality (PQ) of the system.

To evaluate the effectiveness of the proposed method, simulations are conducted using a practical system. The simulation results demonstrate that the overall voltage and current harmonics are significantly reduced when compared to traditional modulation techniques. This reduction in harmonics leads to enhanced power quality, which is a desirable outcome in power electronic or sensitive based systems. The proposed method combines the BBO algorithm with the SHE-PWM technique to optimize switching angles for inverters, aiming to eliminate lower order harmonics and improve power quality. The simulation results validate the effectiveness of this approach by showcasing reduced harmonics for minimum %THD and enhanced power quality in a practical system.

Selected Harmonic Elimination Pulse Width Modulation (SHE-PWM) is a technique used in power electronics inverter control circuit and electric power systems. It aims to control the switching patterns of power electronic devices such as inverters, allowing them to generate high-quality output waveforms with reduced harmonic content.

When these two techniques are combined, we get the BBO-based SHE-PWM technique, which leverages the BBO algorithm to optimize the selection of switching angles or pulse widths in SHE-PWM. By applying BBO, the technique searches for the optimal set of switching angles that minimizes the total harmonic distortion (THD) of the output waveform, thereby improving the performance of the overall system.

The BBO algorithm starts with an initial population of candidate solutions, which are encoded as vectors representing the switching angles or pulse widths. These solutions are evaluated based on an objective function, which calculates the THD of the resulting waveform. The BBO algorithm then applies migration and mutation operators inspired by the principles of biogeography to explore and exploit the search space, aiming to find the optimal solution.

Through iterations and generations, the BBO algorithm updates the population by exchanging and modifying solutions, ultimately converging towards the best set of switching angles that minimizes % THD. The BBO-based SHE-PWM technique provides an efficient and effective way to achieve optimal harmonic elimination in the proposed systems.

Overall, the BBO-based SHE-PWM technique combines the power of the BBO algorithm's search and optimization capabilities with the objective of reducing harmonic distortion in the proposed systems, leading to improved system performance and reduced power losses.

3.1. 180° mode of operation for proposed UPQC model

The instantaneous phase voltage of the inverter output V_{aN_phase} (for one phase from Fig. 2) generally expressed in a Fourier series form as,

$$V_{aN\_phase} = \frac{a_0}{2} + \sum_{N=1}^{\infty}\left(a_{N\_har\_coef}\cos(N\omega t) + b_{N\_har\_coef}\sin(N\omega t)\right) \quad (1)$$

Consequently, if the output wave form has quarter-wave symmetry (Fig. 2), we obtain

$a_0 = 0$ for all N, and $a_{N\_har\_coef} = 0$, for all even N

The phase voltage Eq. (1) becomes

$$V_{aN\_phase} = \sum_{N=1}^{\infty}\left(b_{N\_har\_coef}\sin(N\omega t)\right)$$

$$b_{N\_har\_coef} = \frac{4}{\pi}\int_0^{\pi/2} e(\omega t)\sin(N\omega t)d(\omega t) \text{ for all odd } 'N' \text{ or, } b_{N\_har\_coef} =$$

$$\frac{4}{\pi}\left[\int_0^{\pi/3}\frac{V_{dc}}{3}\sin(N\omega t)d(\omega t) + \int_{\pi/3}^{\pi/2}\frac{2V_{dc}}{3}\sin(N\omega t)d(\omega t)\right]$$

$$= \frac{4V_{dc}}{3N\pi}\left[\left[\cos(N\omega t)\right]_{\pi/3}^{0} + 2\left[\cos(N\omega t)\right]_{\pi/2}^{\pi/3}\right]$$

$$= \frac{4V_{dc}}{3N\pi}\left[1 - \cos\left(\frac{N\pi}{3}\right) + 2\cos\left(\frac{N\pi}{3}\right) - 2\cos\left(\frac{N\pi}{2}\right)\right]$$

but, $\cos\left(\frac{N\pi}{2}\right) = 0$ for all odd N,

The mathematical formula for the Nth harmonic component is $b_{N\_har\_coef} = \frac{4V_{dc}}{3N\pi}\left[1 + \cos\left(\frac{N\pi}{3}\right)\right]$ and the measured phase angle is

$$\phi_N = \tan^{-1}\left(\frac{a_{N\_har\_coef}}{b_{N\_har\_coef}}\right) = 0 \quad (2)$$

where, $a_{N\_har\_coef} = 0$.

Looking at Eq. (2), we notice that triple-N harmonics (3, 9, 12, 15, ⋯) are naturally nullified in a balanced three-phase system. Consequently, we don't target the elimination of triple-N harmonics in phase voltages. Analyzing the phase voltage waveform for harmonics reveals the presence of Nth harmonics where N takes values such as 1, 5, 7, 11, 13, 17, ⋯ or can be expressed as N = 6 k ± 1 for k = 1, 2, 3, 4, ⋯.

So, the actual phase voltage equation becomes

$$V_{aN\_phase} = \sum_{N=1}^{\infty}\frac{4V_{dc}}{3N\pi}\left[1 + \cos\left(\frac{N\pi}{3}\right)\right]\sin(N\omega t)$$

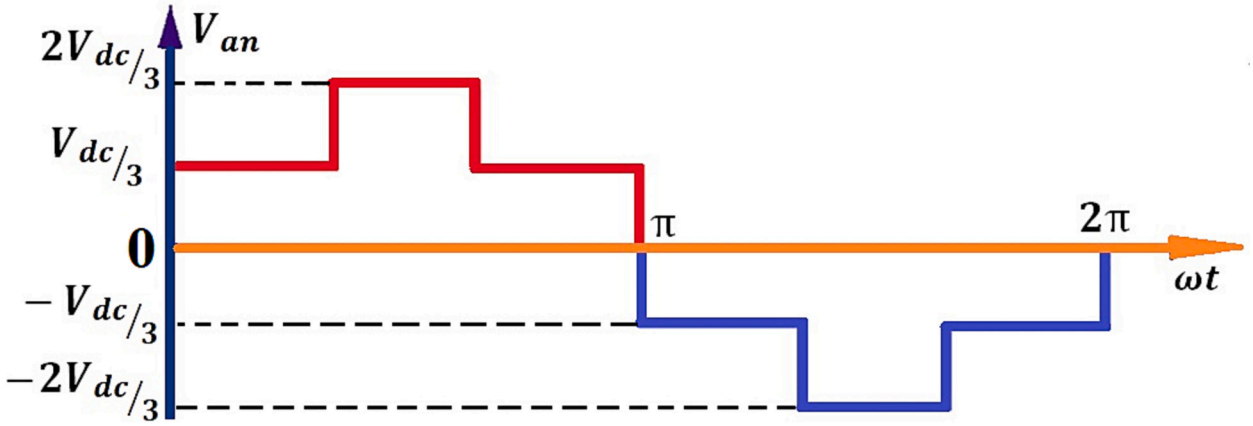

Fig. 2. A 3-ϕ output Quasi-sine waveforms of 180° inverter phase voltage (one phase) applied to the grid, micro-grid or smart grid system.

The phase voltage switching pattern for six-step quasi-sine waveforms in 180° conduction mode is depicted in Fig. 3.

A three-phase bridge inverter's phase voltage (Fig. 3) waveform is a quasi-square wave. The wave form exhibits quarter-wave symmetry, and as a result of the

$a_0 = 0$ for all N, and $a_{\mathrm{N\_har\_coef}} = 0$, for all even $'N'$

then, $V_{aN\_phase} = \sum_{N=1,5,7,\ldots}^{\infty} b_{bN\_har\_coef} sin(N\omega t)$

or, $b_{N\_har\_coef} = \frac{1}{\pi}\int_0^{2\pi} V_{aN\_phase} sin(N\omega t) d(\omega t)$

$$= \frac{4}{\pi}\int_0^{\pi/2} V_{aN\_phase} sin(N\omega t) d(\omega t)$$

$$= \frac{4}{\pi}\left[\int_{\alpha_{1st}}^{\alpha_{2nd}} V_{aN\_phase} sin(N\omega t) d(\omega t) + \int_{\alpha_{3rd}}^{\alpha_{4th}} V_{aN\_phase} sin(N\omega t) d(\omega t) + \int_{\alpha_{5th}}^{\pi/2} V_{aN\_phase} sin(N\omega t) d(\omega t)\right]$$

$$= \frac{4}{\pi}\left[\int_{\alpha_{1st}}^{\alpha_{2nd}} \frac{V_{dc}}{3} sin(N\omega t) d(\omega t) + \int_{\alpha_{3rd}}^{\alpha_{4th}} \frac{V_{dc}}{3} sin(N\omega t) d(\omega t) + \int_{\alpha_{5th}}^{\pi/2} \frac{2V_{dc}}{3} sin(N\omega t) d(\omega t)\right]$$

$$= \frac{4V_{dc}}{3N\pi}\left[(-1)cos(N\omega t)\,|_{\alpha_{1st}}^{\alpha_{2nd}} + (-1)cos(N\omega t)\,|_{\alpha_{3rd}}^{\alpha_{4th}} + 2(-1)cos(N\omega t)\,|_{\alpha_{5th}}^{\pi/2}\right]$$

$$= \frac{4V_{dc}}{3N\pi}[\mathrm{cosN}\alpha_1 - \mathrm{cosN}\alpha_2 + \mathrm{cosN}\alpha_3 - \mathrm{cosN}\alpha_4 + 2\mathrm{cosN}\alpha_5 - 2cosN\pi/2]$$

$cosN\pi/2 = 0$ for $N = 1, 5, 7, 11, \cdots, (6N \pm 1)$

$$= \frac{4V_{dc}}{3N\pi}[\mathrm{cosN}\alpha_{1st} - \mathrm{cosN}\alpha_{2nd} + \mathrm{cosN}\alpha_{3rd} - \mathrm{cosN}\alpha_{4th} + 2\mathrm{cosN}\alpha_{5th}]$$

Put $N = 1, 5, 7, 11, 13, \cdots$ the harmonic coefficient can be easily calculated and which is,

$$b_{1\_har\_coef} = \frac{4V_{dc}}{3\pi}[cos1\alpha_{1st} - cos1\alpha_{2nd} + cos1\alpha_{3rd} - cos1\alpha_{4th} + 2cos1\alpha_{5th}]$$

$$b_{5\_har\_coef} = \frac{4V_{dc}}{3\times 5\times \pi}[cos5\alpha_{1st} - cos5\alpha_{2nd} + cos5\alpha_{3rd} - cos5\alpha_{4th} + 2cos5\alpha_{5th}]$$

$$b_{7\_har\_coef} = \frac{4V_{dc}}{3\times 7\times \pi}[cos7\alpha_{1st} - cos7\alpha_{2nd} + cos7\alpha_{3rd} - cos7\alpha_{4th} + 2cos7\alpha_{5th}]$$

Thus, the general equation of $b_{n\_\mathrm{har\_coef}}$ can be written as Eq. (3),

$$b_{\mathrm{N\_har\_coef}} = \frac{4V_{dc}}{3N\pi}\left[-\sum_{k=1}^{m}(-1)^k cos(N\alpha_k) - 2\sum_{k=m+1}^{N}(-1)^k cos(N\alpha_k)\right]$$

or

$$V_{aN\_phase} = \frac{4V_{dc}}{3N\pi}\left[-\sum_{k=1}^{m}(-1)^k cos(N\alpha_k) - 2 \times \sum_{k=m+1}^{N}(-1)^k cos(N\alpha_k)\right] sin(\mathrm{N}\omega t) \quad (3)$$

For 5-switching, the measured statement of these situations is expressed as Eq. (4)

$$\begin{cases} cos\alpha_{1st} - cos\alpha_{2nd} + cos\alpha_{3rd} - cos\alpha_{4th} + 2cos\alpha_{5th} = \mathrm{M} \\ cos5\alpha_{1st} - cos5\alpha_{2nd} + cos5\alpha_{3rd} - cos5\alpha_{4rd} + 2cos5\alpha_{5th} = 0 \\ cos7\alpha_{1st} - cos7\alpha_{2nd} + cos7\alpha_{3rd} - cos7\alpha_{4th} + 2cos7\alpha_{5th} = 0 \\ cos11\alpha_{1st} - cos11\alpha_{2nd} + cos11\alpha_{3rd} - cos11\alpha_{4th} + 2cos11\alpha_{5th} = 0 \\ cos13\alpha_{1st} - cos13\alpha_{2nd} + cos13\alpha_{3rd} - cos13\alpha_{th} + 2cos13\alpha_{5th} = 0 \end{cases} \quad (4)$$

The 5*th*,7*th*, 11*th* and 13*th* order of inverter generated harmonics would be eliminated if $b_{5\_har\_coef} = b_{7\_har\_coef} = b_{11\_har\_coef} = b_{13\_har\_coef} =$

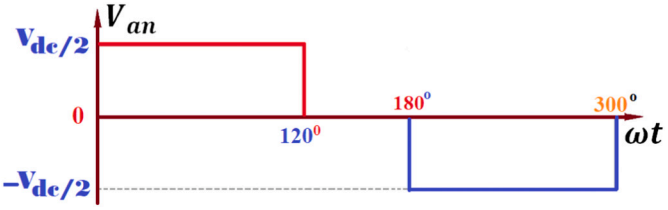

Fig. 4. 3-phase Quasi-sine waveforms of 120° switch conduction phase voltage applied to the UPQC.

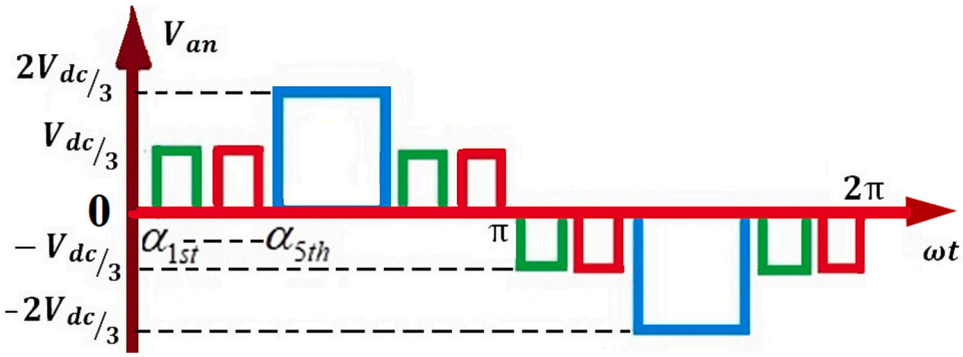

Fig. 3. A 3-ϕ six-step Quasi-sine voltage waveforms of 180° conduction mode with five (α_1 toα_5) switching angles.

0. These nonlinear equations can be resolved iteratively and compute the α_{1st}, α_{2nd}, α_{3rd}, ⋯ α_{kth} for low % THD.

Similarly for 3-switching the inverter output phase voltage switching design and calculate the harmonics. For elimination of the 5*th* and 7*th* lower order harmonics, $b_{5\_har\_coef} = b_{7\_har\_coef} = 0$; where the total number of switching angles = 3. Three notches per quarter-wave would be required. Eq. (5) is the set of nonlinear simultaneous equations to solve for the angles.

$$\begin{cases} cos\alpha_{1st} - cos\alpha_{2nd} + 2cos\alpha_{3rd} = \mathrm{M} \\ cos5\alpha_{1st} - cos5\alpha_{2nd} + 2cos5\alpha_{3rd} = 0 \\ cos7\alpha_{1st} - cos7\alpha_{2nd} + 2cos7\alpha_{3rd} = 0 \\ cos11\alpha_{1st} - cos11\alpha_{2nd} + 2cos11\alpha_{3rd} = 0 \\ cos13\alpha_{1st} - cos13\alpha_{2nd} + 2cos13\alpha_{3rd} = 0 \end{cases} \quad (5)$$

3.2. 120° mode of operation for proposed UPQC model

Fig. 4 displays the 3-phase instantaneous quasi-sine waveforms of switch conduction phase voltage applied to the Unified Power Quality Conditioner (UPQC).

The N^{th} number of harmonic components can be mathematically expressed as Eq. (6)

$$b_{\mathrm{N\_har\_coef}} = \frac{2V_{dc}}{N\pi} sin\left(\frac{N\pi}{2}\right) sin\left(\frac{N\pi}{3}\right), \text{where } sin\left(\frac{n\pi}{3}\right) = cos\left(\frac{n\pi}{6}\right) \quad (6)$$

and $\phi_N = tan^{-1}\left(\frac{a_{\mathrm{N\_har\_coef}}}{b_{\mathrm{N\_har\_coef}}}\right) = 0$

3.2.1. Proposed switching strategy for 120° mode of operation

In a three-phase bridge inverter, the phase voltage waveform is typically a quasi-square wave, which means it consists of six steps or levels. This waveform is achieved by switching the power devices (such as transistors or thyristors) in a specific pattern. Each phase of the inverter operates with a 120-degree phase shift from the others.

The term "quasi-square wave" implies that the waveform approximates a square wave but is not perfectly square due to switching and circuit limitations. However, it still exhibits certain characteristics of a square wave.

The waveform mentioned in Fig. 5 is likely a representation of the six-step quasi-sine waveforms of the 120-degree switch conduction phase voltage waveform. These waveforms have quarter-wave symmetry, meaning they repeat every quarter of the fundamental period.

When it comes to the isolated neutral-phase voltages, they also follow a six-step waveform pattern. However, the fundamental component of these voltages is phase-shifted by pi/6 (30 degrees) from the respective line voltage. This phase shift ensures the balanced operation of the three-phase system.

Additionally, the triple-n harmonics, which are undesirable harmonics at frequencies that are multiples of the fundamental frequency, are suppressed in this case. The specific design or control techniques employed in the inverter help to reduce or eliminate these harmonics, resulting in a cleaner output waveform.

It's worth noting that the exact details of the waveform and its characteristics can vary depending on the specific design and control strategy implemented in the three-phase bridge inverter.

$a_0 = 0$ for all N, and $a_{\mathrm{N\_har\_coef}} = 0$, for all even $'N'$

$$b_{\mathrm{N\_har\_coef}} = \frac{1}{\pi}\int_0^{2\pi} V_{aN\_phase} sin(N\omega t)d(\omega t)$$

$$b_{\mathrm{N\_har\_coef}} = \frac{4}{\pi}\int_0^{\pi/2} V_{aN\_phase} sin(N\omega t)d(\omega t)$$

$$= \frac{4}{\pi}\left[\int_{\alpha_{1st}}^{\alpha_{2nd}} V_{aN\_phase} sin(N\omega t)d(\omega t) + \int_{\alpha_{3rd}}^{\alpha_{4th}} V_{aN\_phase} sin(N\omega t)d(\omega t) + \int_{\alpha_{5th}}^{\pi/2} V_{aN\_phase} sin(N\omega t)d(\omega t)\right]$$

$$= \frac{4}{\pi}\left[\int_{\alpha_{1st}}^{\alpha_{2nd}} \frac{V_{dc}}{2} sin(N\omega t)d(\omega t) + \int_{\alpha_{3rd}}^{\alpha_{4th}} \frac{V_{dc}}{2} sin(N\omega t)d(\omega t) + \int_{\alpha_{5th}}^{\pi/2} \frac{V_{dc}}{2} sin(N\omega t)d(\omega t)\right]$$

$$= \frac{4V_{dc}}{2N\pi}\left[(-1)cos(\mathrm{N}\omega t)\,|_{\alpha_{1st}}^{\alpha_{2nd}} + (-1)cos(\mathrm{N}\omega t)\,|_{\alpha_{3rd}}^{\alpha_{4th}} + (-1)cos(\mathrm{N}\omega t)\,|_{\alpha_{5th}}^{\pi/2}\right]$$

$$= \frac{2V_{dc}}{N\pi}[\mathrm{cosN}\alpha_{1st} - \mathrm{cosN}\alpha_{2nd} + \mathrm{cosN}\alpha_{3rd} - \mathrm{cosN}\alpha_{4th} + \mathrm{cosN}\alpha_{5th} - \mathrm{cosN}\pi/2]$$

$$= \frac{2V_{dc}}{N\pi}[\mathrm{cosN}\alpha_{1st} - \mathrm{cosN}\alpha_{2nd} + \mathrm{cosN}\alpha_{3rd} - \mathrm{cosN}\alpha_{4th} + \mathrm{cosN}\alpha_{5th}]$$

$$\mathrm{cosN}\pi/2 = 0, for, \mathrm{N} = 1,5,7,11,\cdots upto(6N \pm 1)$$

The expression for $b_{N\_har\_coef}$ can be written as Eq. (7),

$$b_{n\_har\_coef} = -\left(\frac{2V_{dc}}{N\pi}\right)\sum_{k=1}^{m}(-1)^k cos(N\alpha_k)$$

Or, the phase voltage is

$$V_{an\_phase} = -\left(\frac{2V_{dc}}{N\pi}\right)\left[\sum_{k=1}^{m}(-1)^k cos(N\alpha_k)\right] sin(\mathrm{N}\omega t) \quad (7)$$

Put $k = 1,5,7,11,13,\cdots$

$$b_{1st\_har\_coef} = \frac{2V_{dc}}{\pi}[cos1\alpha_{1st} - cos1\alpha_{2nd} + cos1\alpha_{3rd} - cos1\alpha_{4th} + cos1\alpha_{5th}]$$

$$b_{5th\_har\_coef} = \frac{2V_{dc}}{5\pi}[cos5\alpha_{1st} - cos5\alpha_{2nd} + cos5\alpha_{3rd} - cos5\alpha_{4th} + cos5\alpha_{5th}]$$

$$b_{7th\_har\_coef} = \frac{2V_{dc}}{7\pi}[cos7\alpha_{1st} - cos7\alpha_{2nd} + cos7\alpha_{3rd} - cos7\alpha_{4th} + cos7\alpha_{5th}]$$

The mathematical formulation of these circumstances is then Eq. (8) for 5-switching.

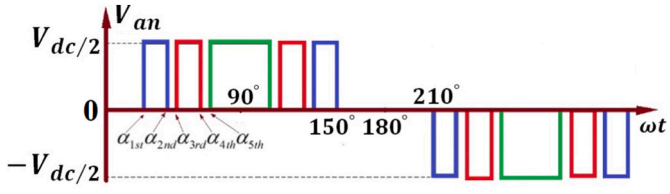

Fig. 5. Three-phase quasi-sine voltage switching waveforms with a 120° switch conduction phase, five switching angles, and a 30° phase beginning point.

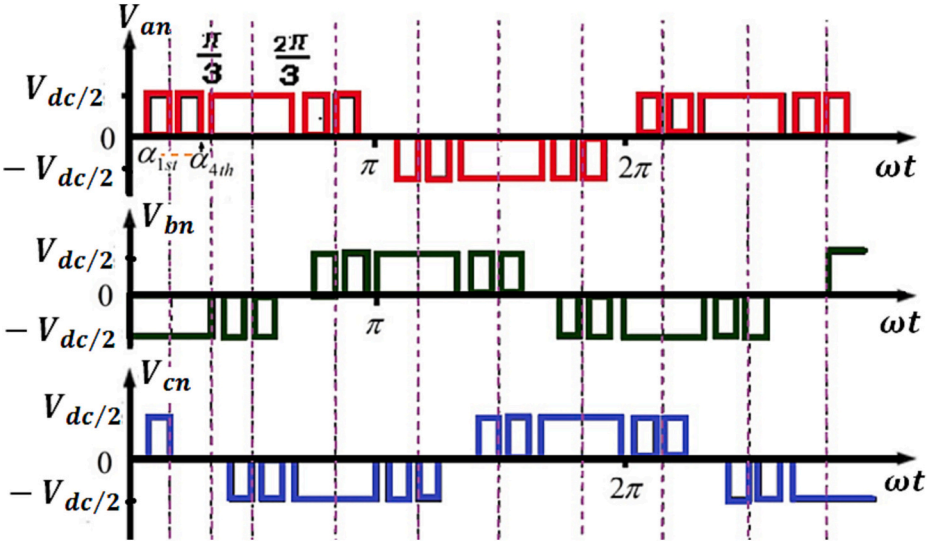

Fig. 6. A 120-degree switch conduction, three-phase, six-step, modified phase voltage switching pattern.

$$\begin{cases} cos\alpha_{1st} - cos\alpha_{2nd} + cos\alpha_{3rd} - cos\alpha_{4th} + cos\alpha_{5th} = \mathrm{M} \\ cos5\alpha_{1st} - cos5\alpha_{2nd} + cos5\alpha_{3rd} - cos5\alpha_{4th} + cos5\alpha_{5th} = 0 \\ cos7\alpha_{1st} - cos7\alpha_{2nd} + cos7\alpha_{3rd} - cos7\alpha_{4th} + cos7\alpha_{5th} = 0 \\ cos11\alpha_{1st} - cos11\alpha_{2nd} + cos11\alpha_{3rd} - cos11\alpha_{4th} + cos11\alpha_{5th} = 0 \\ cos13\alpha_{1st} - cos13\alpha_{2nd} + cos13\alpha_{3rd} - cos13\alpha_{4th} + cos13\alpha_{5th} = 0 \end{cases} \quad (8)$$

$$b_{\mathrm{N}\_har\_coef} = \frac{4}{\pi}\int_{0}^{\pi/2} V_{aN\_phase} sin(N\omega t)d(\omega t)$$

$$= \frac{4}{\pi}\left[\int_{\alpha_{1th}}^{\alpha_{2nd}} V_{aN\_phase} sin(N\omega t)d(\omega t) + \int_{\alpha_{3rd}}^{\alpha_{4th}} V_{aN\_phase} sin(N\omega t)d(\omega t) + \int_{\alpha_{5th}}^{\alpha_{6th}} V_{aN\_phase} sin(N\omega t)d(\omega t) + \int_{\pi/3}^{\pi/2} V_{aN\_phase} sin(N\omega t)d(\omega t)\right]$$

$$= \frac{4}{\pi}\left[\int_{\alpha_{1st}}^{\alpha_{2nd}} \frac{V_{dc}}{2} sin(N\omega t)d(\omega t) + \int_{\alpha_{3rd}}^{\alpha_{4th}} \frac{V_{dc}}{2} sin(N\omega t)d(\omega t) + \int_{\alpha_{5th}}^{\alpha_{6th}} \frac{V_{dc}}{2} sin(N\omega t)d(\omega t) + \int_{\pi/3}^{\pi/2} \frac{V_{dc}}{2} sin(N\omega t)d(\omega t)\right]$$

The $5^{th}, 7^{th}, 11^{th}$ and 13^{th} order of harmonics would be eliminated if $b_{5th\_har\_coef} = b_{7th\_har\_coef} = b_{11\eta\_har\_coef} = b_{13\eta\_har\_coef} = 0$ and the higher order harmonic would be suppressed by proper choice of switching angle.

3.3. 60° modulation technique for proposed UPQC

Fig. 6 displays a three-phase six-step quasi-sine waveform with 120° switch conduction MODIFIED phase voltage.

In a 3-phase bridge inverter, the phase voltage waveform can be approximated as a quasi-square wave. It has quarter-wave symmetry, meaning that the positive and negative half-cycles of the waveform are symmetrical and repeated every quarter-cycle.

The quasi-square wave can be expressed as a summation of odd harmonics. The fundamental frequency ω corresponds to the first harmonic, and the subsequent odd harmonics are integer multiples of the fundamental frequency. The phase voltage waveform of a 3-phase bridge inverter is a quasi-square wave. The wave form has quarter-wave symmetry, and

$a_0 = 0$ for all N, and $a_{\mathrm{N}\_har\_coef} = 0$, for all even $'N'$

$$b_{\mathrm{N}\_har\_coef} = \frac{1}{\pi}\int_{0}^{2\pi} V_{aN\_phase} sin(N\omega t)d(\omega t)$$

$$= \frac{4V_{dc}}{2N\pi}\left[(-1)cos(\mathrm{N}\omega t)\,|_{\alpha_{1st}}^{\alpha_{2nd}} + (-1)cos(\mathrm{N}\omega t)\,|_{\alpha_{3rd}}^{\alpha_{4th}} + (-1)cos(\mathrm{N}\omega t)\,|_{\alpha_{5th}}^{\alpha_{6th}} + (-1)cos(\mathrm{N}\omega t)\,|_{\pi/2}^{\pi/2}\right]$$

$$= \frac{2V_{dc}}{N\pi}[\mathrm{cosN}\alpha_{1st} - \mathrm{cosN}\alpha_{2nd} + \mathrm{cosN}\alpha_{3rd} - \mathrm{cosN}\alpha_{4th} + \mathrm{cosN}\alpha_{5th} - \mathrm{cosN}\alpha_{6th} + \mathrm{cosN}\pi/3 - \mathrm{cosN}\pi/2]$$

$$\mathrm{cosN}\pi/2 = 0, for, \mathrm{N} = 1, 5, 7, 11, \cdots upto(6N \pm 1)$$

$$= \frac{2V_{dc}}{N\pi}\left[\frac{1}{2} + \mathrm{cosN}\alpha_{1st} - \mathrm{cosN}\alpha_{2nd} + \mathrm{cosN}\alpha_{3rd} - \mathrm{cosN}\alpha_{4th} + \mathrm{cosN}\alpha_{5th} - \mathrm{cosN}\alpha_{6th}\right]$$

The expression for $b_{n\_har\_coef}$ can be written as Eq. (9),

$$b_{\mathrm{N}\_har\_coef} = \left(\frac{2V_{dc}}{N\pi}\right)\left[\sum_{k=1}^{m}\frac{1}{2} - (-1)^k cos(N\alpha_k)\right] \quad (9)$$

Put $k = 1, 5, 7, 11, 13, \cdots$

$$b_{1st\_har\_coef} = \frac{2V_{dc}}{\pi}\left[\frac{1}{2} + cos1\alpha_{1st} - cos1\alpha_{2nd} + cos1\alpha_{3rd} - cos1\alpha_{4th} + cos1\alpha_{5th} - cos1\alpha_{6th}\right]$$

$$b_{5th\_har\_coef} = \frac{2V_{dc}}{5\pi}\left[\frac{1}{2} + cos5\alpha_{1st} - cos5\alpha_{2nd} + cos5\alpha_{3rd} - cos5\alpha_{4th} + cos5\alpha_{5th} - cos5\alpha_{6th}\right]$$

$$b_{7th\_har\_coef} = \frac{2V_{dc}}{7\pi}\left[\frac{1}{2} + cos7\alpha_{1st} - cos7\alpha_{2nd} + cos7\alpha_{3rd} - cos7\alpha_{4th} + cos7\alpha_{5th} - cos7\alpha_{6th}\right]$$

For 5-switching, the mathematical statement of these circumstances is then Eq. (10)

$$\begin{cases} \frac{1}{2} + cos\alpha_{1st} - cos\alpha_{2nd} + cos\alpha_{3rd} - cos\alpha_{4th} + cos\alpha_{5th} - cosn\alpha_{6th} = \mathrm{M} \\ \frac{1}{2} + cos5\alpha_{1st} - cos5\alpha_{2nd} + cos5\alpha_{3rd} - cos5\alpha_{4th} + cos5\alpha_{5th} - cosn\alpha_{6th} = 0 \\ \frac{1}{2} + cos7\alpha_{1st} - cos7\alpha_{2nd} + cos7\alpha_{3rd} - cos7\alpha_{4th} + cos7\alpha_{5th} - cosn\alpha_{6th} = 0 \\ \frac{1}{2} + cos11\alpha_{1st} - cos11\alpha_{2nd} + cos11\alpha_{3rd} - cos11\alpha_{4th} + cos11\alpha_{5th} - cosn\alpha_{6th} = 0 \\ \frac{1}{2} + cos13\alpha_{1st} - cos13\alpha_{2nd} + cos13\alpha_{3rd} - cos13\alpha_{4th} + cos13\alpha_{5th} - cosn\alpha_{6th} = 0 \end{cases} \quad (10)$$

The 5^{th},7^{th},11^{th} and 13^{th} order of harmonics would be eliminated if$b_{5th.har.coef} = b_{7th.har.coef} = b_{11th.har.coef} = b_{13th.har.coef} = 0$ and the higher order harmonic would be suppressed by proper choice of switching angles.

For 3-switching the nonlinear equation is Eq. (11)

$$\begin{cases} cos\alpha_{1st} - cos_{2nd} + cos\alpha_{3rd} = M \\ cos5\alpha_{1st} - cos5\alpha_{2nd} + cos5\alpha_{3rd} = 0 \\ cos7\alpha_{1st} - cos7\alpha_{2nd} + cos7\alpha_{3rd} = 0 \end{cases} \quad (11)$$

The 5*th* and 7*th* harmonics would be eliminated if $b_{5th\_har\_coef} = b_{7th\_har\_coef} = 0$.These equations can be solved iteratively and calculate the switching angles α_{1st}, α_{2nd} and α_{3rd}. The Biogeography-Based Optimization (BBO)-based Selected Harmonic Elimination Pulse Width Modulation (SHE-PWM) technique is an optimization method used to determine the optimal switching angles for Pulse Width Modulation (PWM) in power electronic inverter systems.

It combines the BBO algorithm with the SHE-PWM technique to achieve improved performance and reduced harmonic distortion. In Tables 1 and 2 the calculation of inverter switching angles for different order harmonic elimination with 180- degree and 120-degree conduction mode.

In the SHE-PWM technique, the objective is to eliminate or minimize specific harmonics in the output waveform generated by power electronic devices, such as inverters. This is accomplished by strategically selecting the switching angles or pulse widths of the power electronic devices. By controlling the switching angles, it is possible to manipulate the harmonic content and achieve a desired output waveform with reduced harmonics.

The BBO algorithm, inspired by biogeography, provides an optimization framework to determine the optimal set of switching angles that minimizes harmonic distortion. It mimics the migration and distribution patterns of species in biological systems to explore and exploit the solution space. The BBO algorithm utilizes concepts such as immigration, emigration, and mutation to iteratively search for the optimal solution.

In the BBO-based SHE-PWM technique, the BBO algorithm is employed to search for the best set of switching angles that minimizes harmonic distortion, typically measured using metrics like Total Harmonic Distortion (THD). The algorithm starts with an initial population of candidate solutions, representing different sets of switching angles. These solutions are evaluated based on the objective function, which calculates the THD of the output waveform. Through successive iterations and updates, the BBO algorithm refines the population to converge towards the optimal solution.

By integrating the BBO algorithm into the SHE-PWM technique, the BBO-based SHE-PWM technique offers a powerful optimization approach for determining the switching angles that lead to minimized harmonic distortion. It improves the overall power quality and performance of the system, resulting in better efficiency, reduced losses, and improved operation.

4. MATLAB simulation results

4.1. Balanced and unbalanced voltage sags and swells mitigation for linear and nonlinear load

Case study 1:

In Fig. 7 provides an in-depth analysis of the output voltage sag response in a ZS-PV-FC-based UPQC system. This configuration is designed to address a balanced fault in the R-phase, Y-phase, B-phase, and ground, employing 3-switching for harmonic elimination (specifically targeting the 5th and 7th harmonics). The subplots in Fig. 7 illustrate:

a. **Supply Side Voltage Waveform (Balanced 3-ϕ Fault):** This plot reveals the voltage waveform on the supply side during a balanced 3-phase fault, serving as a baseline for understanding the impact of subsequent events.
b. **Injected Voltage by the Proposed UPQC:** The UPQC is initiated at t = 0.1 s (a voltage dip between t = 0.1 s to the interval t = 0.26 s), with the FC-PV-Battery-Z source and BBO-based technology. This subplot showcases the injected voltage by the UPQC, demonstrating its ability to counteract the voltage dip caused by the 3-phase fault.
c. **3-Phase Non-Linear Load Voltage Waveform:** This subplot displays the voltage waveform of the R-L-C non-linear sensitive load, emphasizing the impact of the fault on the load and how the UPQC intervention influences this waveform.

Detailed discussions:

i. **Fault Occurrence and UPQC Activation:** At t = 0.1 s, the 3-phase fault occurs in the grid, triggering the UPQC into operation. The source voltage at this moment is 230 V, and the UPQC swiftly responds to the fault-induced voltage dip.
ii. **Modulation Index and Switching Angles:** The modulation index is set at 0.88 during this operation. The specified switching angles (14.6442, 78.432, 86.7606 degrees) for the 180-degree conduction mode indicate the precise moments at which the UPQC modulates its output to rectify the voltage disturbances.
iii. **Harmonic Elimination and THD Reduction:** Employing 3-switching, the UPQC successfully eliminates the 5th and 7th order harmonics. Without a filter, the total harmonic distortion (%THD) is 4.9376, but with a filter, it reduces significantly to 2.31. This highlights the efficacy of the UPQC in enhancing power quality by reducing harmonic content.

Waveform Analysis:

(1) **Supply Side Voltage:** Observe how the fault affects the supply side voltage and how the UPQC injects corrective voltage to mitigate the sag.
(2) **Injected Voltage:** Analyze the waveform of the voltage injected by the UPQC, emphasizing its rapid response and effectiveness in stabilizing the voltage during the fault period.

Table 1
Calculation of inverter switching angles for different order harmonic elimination with 180-degree conduction mode.

MI	alpha1	alpha2	alpha3	% THD	Harmonic elimination
0.1	58.36	61.67	88.57	41.27	5th harmonic and 7th order harmonic elimination by 3-switching
0.2	56.88	63.18	87.29	39.74	
0.3	55.06	65.07	85.71	37.81	
0.4	53.42	66.84	84.32	34.66	
0.5	51.45	69.08	82.72	29.02	
0.6	50.12	70.74	81.71	27.82	
0.7	48.46	73.21	80.61	13.34	
0.8	46.74	77.43	80.43	11.06	
0.91	15.24	82.91	88.04	8.69	

MI	alpha1	alpha2	alpha3	alpha 4	% THD	Harmonic elimination
0.1	53.992	56.357	78.984	86.420	38.043	5th harmonic, 7th harmonic and 11th harmonic elimination by 4-switching
0.2	52.545	57.125	75.741	86.810	34.296	
0.3	51.153	57.787	73.049	87.530	28.209	
0.4	49.764	58.201	70.410	88.430	17.834	
0.5	11.210	60.494	77.078	84.480	14.673	
0.6	12.018	61.890	74.587	85.050	12.132	
0.7	25.708	40.913	53.229	88.730	10.417	
0.8	18.757	46.886	52.331	87.850	9.122	
0.87	15.344	60.192	61.820	88.010	7.302	

MI	alpha1	alpha2	alpha3	alpha 4	alpha 5	% THD	Harmonic elimination
0.11	49.143	50.797	68.431	71.560	88.952	25.422	5th harmonic, 7th harmonic, 11th harmonic and 13th order harmonic elimination by 5-switching
0.2	48.408	51.388	67.116	72.852	88.103	19.866	
0.3	7.363	15.592	42.782	56.431	87.408	14.022	
0.39	46.760	52.330	64.132	75.761	86.396	13.169	
0.51	45.630	52.509	61.929	77.966	85.490	11.800	
0.6	44.680	52.162	59.902	80.278	85.131	8.109	
0.7	16.623	50.774	56.945	77.284	88.600	6.826	
0.78	18.694	47.218	53.070	83.549	89.327	5.116	

MI	alpha1	alpha2	alpha3	alpha 4	alpha 5	alpha6	alpha7	% THD	Harmonic elimination
0.1	44.702	45.706	59.345	60.897	74.323	76.170	89.286	23.524	5th harmonic, 7th harmonic, 11th harmonic, 13th harmonic, 17th harmonic and
0.2	44.501	45.786	58.712	61.390	73.916	77.134	88.811	16.209	19th order harmonic elimination
0.3	43.693	46.085	57.452	61.964	72.958	78.862	87.876	13.504	
0.4	43.317	46.466	56.466	62.432	71.831	79.462	87.413	11.175	
0.5	42.734	46.701	54.934	62.692	70.779	79.989	86.866	9.632	
0.6	41.431	46.835	53.431	62.782	68.302	79.278	85.900	8.080	
0.7	34.962	43.553	52.071	63.138	65.848	78.677	85.138	7.596	
0.8	24.873	34.341	41.191	63.804	66.225	79.976	85.136	6.426	
0.9	14.581	25.501	29.953	71.347	75.901	84.947	86.869	5.094	
0.91	10.207	23.997	25.144	75.919	76.898	86.952	89.948	4.496	

(3) **Non-Linear Load Voltage:** Assess the response of the R-L-C non-linear sensitive load, considering how the UPQC intervention influences the load's voltage waveform.

In conclusion, the proposed model effectively regulates the balanced 3-phase voltage and rapidly injects the necessary voltage to maintain the critical load. The harmonic elimination and THD reduction further highlight the system's capability to enhance power quality in the presence of grid faults.

Case study 2:

In Fig. 8 captures the response of the ZS-PV-FC-based UPQC to output voltage sag, addressing a balanced fault in the R-phase, Y-phase, B-phase, and ground. The scenario involves 5-switching for harmonic elimination (specifically targeting the 5th, 7th, 11th, and 13th order harmonics). The subplots detail:

a. **Supply Side Voltage Waveform (Balanced 3-ϕ Fault):** This plot outlines the voltage waveform on the supply side during a balanced 3-phase fault, providing a baseline for understanding the impact of subsequent events.
b. **Injected Voltage by the Proposed UPQC:** The UPQC injects corrective voltage starting at t = 0.1 s, utilizing a combination of FC-PV-Battery-Z source and BBO-based technology. This injected voltage is designed to mitigate the effects of the grid failure, and the plot likely exhibits a distinct response during and after the fault.
c. **3-Phase Non-Linear Load Voltage Waveform:** This subplot showcases the voltage waveform of the R-L-C non-linear sensitive load, emphasizing the impact of the fault on the load and how the UPQC intervention influences this waveform.
d. **Fault Occurrence and UPQC Activation:** At t = 0.1 s, a 3-phase grid failure triggers the UPQC into action. The source voltage is 230 V at this moment, and the UPQC commences its corrective operation to counter the ensuing voltage dip.

Table 2
Calculation of inverter switching angles for different order harmonic elimination with 120-degree conduction mode.

MI	alpha1	alpha2	alpha3	% THD	alpha 5	alpha6	alpha7	% THD	Harmonic elimination
0.18	56.873	62.737	84.746	48.857	5th harmonic and 7th order harmonic elimination by 3-switching				
0.2	56.509	62.998	84.134	35.942					
0.32	54.245	64.212	80.170	24.195					
0.4	52.612	64.369	76.976	19.562					
0.5	50.065	62.267	71.129	17.599					
0.6	41.623	48.734	59.201	15.603					
0.7	29.731	39.419	52.832	12.808					
0.8	23.630	38.061	47.840	10.428					
0.9	17.863	33.145	38.233	9.593					

MI	alpha1	alpha2	alpha3	alpha 4	% THD	alpha6	alpha7	Harmonic elimination
0.1	29.632	34.457	64.662	68.123	38.222	5th harmonic, 7th harmonic and 11th harmonic elimination by 4-switching		
0.21	26.913	37.207	62.740	69.924	29.532			
0.31	24.256	39.931	61.034	71.386	17.629			
0.41	21.095	43.276	59.493	72.388	15.509			
0.5	16.559	48.751	59.122	71.796	12.358			
0.6	12.415	60.220	69.293	76.495	11.456			
0.7	13.280	62.444	69.738	80.970	8.834			
0.8	14.399	63.336	67.363	84.989	7.639			
0.87	15.506	58.012	59.602	85.994	6.754			

MI	alpha1	alpha2	alpha3	alpha 4	alpha 5	alpha6	% THD	Harmonic elimination
0.1	21.060	24.269	38.827	42.478	62.881	65.234	36.695	5th harmonic, 7th harmonic, 11th harmonic, 13th harmonic and 17th order harmonic
0.2	19.704	25.359	36.638	43.102	61.733	66.140	24.844	elimination by 6-switching
0.3	17.576	27.163	34.964	46.408	60.650	67.435	17.049	
0.4	15.562	28.027	32.417	48.802	59.783	68.322	10.890	
0.49	15.010	28.633	39.433	53.114	60.016	67.969	9.311	
0.61	16.602	49.518	57.211	71.679	77.089	81.387	8.326	
0.7	15.286	46.292	55.740	74.836	77.797	84.360	7.142	
0.9	9.943	17.331	19.313	72.910	74.183	87.868	6.305	

MI	alpha1	alpha2	alpha3	alpha 4	alpha 5	alpha6	alpha7	% THD	Harmonic elimination
0.1	13.851	16.183	43.423	46.633	59.283	60.923	88.567	25.294	5th harmonic, 7th harmonic, 11th harmonic, 13th harmonic, 17th harmonic and
0.22	12.579	17.647	41.540	48.729	58.830	62.323	86.847	23.678	19th order harmonic elimination
0.31	11.850	18.827	40.061	50.411	58.985	63.734	85.584	19.950	
0.41	11.652	20.447	38.130	52.103	59.646	65.932	84.392	15.130	
0.5	42.070	45.689	54.276	61.410	66.774	77.279	79.821	14.957	
0.6	12.507	21.929	35.965	53.787	59.392	70.338	80.786	13.589	
0.7	22.280	25.675	34.915	40.993	48.314	55.369	59.072	12.693	
0.8	15.491	19.365	27.206	34.634	39.961	50.302	54.166	10.981	
0.9	11.243	16.100	22.705	31.777	34.951	47.888	48.814	4.880	
0.91	10.117	14.225	20.232	44.048	44.817	85.672	87.624	4.759	

- A 3-phase failure in the grid has occurred at time t = 0.1 s, resulting in a voltage dip between t = 0.1 s and the interval t = 0.26 s.

e. **Modulation Index and Switching Angles:** The modulation index is set at 0.88 during this operation. The specified switching angles (18.694, 47.218, 53.07, 83.549, and 89.327 degrees) for the 180-degree conduction mode indicate the precise moments at which the UPQC modulates its output to rectify the voltage disturbances.

f. **Harmonic Elimination:** Through 5-switching, the UPQC effectively eliminates the 5th, 7th, 11th, and 13th order harmonics. This harmonic mitigation strategy ensures a cleaner and more stable power supply.

g. Voltage Waveform Analysis:
- **Supply Side Voltage:** Track how the fault impacts the supply side voltage, observing any deviations and recovery patterns.
- **Injected Voltage:** Analyze the corrective voltage injected by the UPQC, noting its effectiveness in mitigating the sag and restoring stable voltage levels.
- **Non-Linear Load Voltage:** Assess the response of the R-L-C non-linear sensitive load, considering how the UPQC intervention influences the load's voltage waveform.

By scrutinizing these waveforms, we gain insights into the UPQC's ability to maintain grid stability, correct voltage sags, and ensure the quality of power supplied to the sensitive non-linear load and electric vehicle systems.

Case study 3:

Time t = 0.1 s marks the beginning of the operational UPQC using the FC-PV-Battery-Z source and BBO based. At time t = 0.1 s, a 3-phase grid breakdown occurred, causing a voltage dip between t = 0.1 s and the interval t = 0.26 s. The modulation index is then adjusted to 0.88, and the 180-degree conduction mode's computed switching angles are 16.527, 26.507, 31.816, 67.662, 73.539, 83.308 and 85.664-degrees and the % THD is 2.364 by without filter but with filter the % THD is 1.63. For 7-switching, the 5th order, 7th order, 11th order, 13th, 17th and 19th order harmonics are eliminated. Fig. 9 shows the voltage

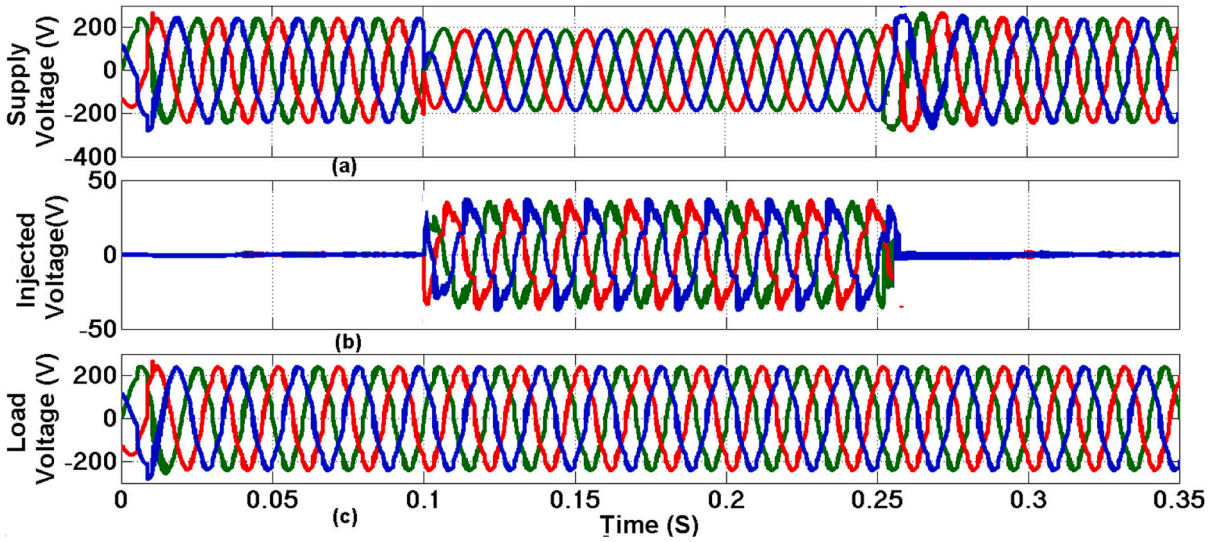

Fig. 7. Output voltage sag response of ZS-PV-FC based UPQC with R-L-C non-linear load (sensitive) and EV load when R-phase, Y-phase, B-phase and ground balanced fault for 3-switching (5th & 7th harmonic elimination) (a) Supply side voltage waveform for balanced 3-ϕ fault (b) by the proposed UPQC injected voltage (c) 3-phase non-linear load voltage waveform.

waveforms with the supply side voltage waveform, the injected voltage from the UPQC, and the R-L-C non-linear sensitive load also the load side extra fault current and the actual load current.

Case study 4:

In Fig. 10, observe the impact of output voltage swells in the response of a ZS-PV-FC-based UPQC when dealing with a capacitive non-linear load (sensitive) and an EV system during a balanced fault in the R-phase, Y-phase, B-phase, and ground. This scenario involves 5-switching for harmonic elimination (specifically, the 5th, 7th, 11th, and 13th harmonics). The subplots illustrate: (a) the supply side voltage waveform during a balanced 3-ϕ fault, (b) the balanced negative-injected voltage achieved by the proposed ZS-FC-PV-UPQC, and (c) the voltage waveform of the 3-phase nonlinear load.

Here, a balanced and unbalanced voltage swell was simulated by attaching a 3-bank of capacitors to the suggested model in order to evaluate the overall effectiveness of the proposed FC-PV-Battery-Z source and BBO based UPQC regulate the voltage swells.

i. **Voltage Swells:**
   - **Waveform Analysis (Fig. 10):** The 3-phase voltage waveforms on the supply side exhibit swells occurring between 0.1 and 0.25 s.
   - **Voltage Increase:** At the moment of swelling, there is a noticeable increase of 76 V, transitioning from 230 V to 306 V.

ii. **Load Voltage Maintenance:**
   - **Effectiveness of UPQC:** Despite the voltage swell, the load voltage is effectively maintained. UPQC plays a crucial role in absorbing the excess swell voltage, preventing disturbances to the connected load.

iii. **Modulation Index Adjustment:**
   - **Optimization for 5-Switching Angles:** The modulation index is fine-tuned to 0.99. The system operates in the 120-degree conduction mode, utilizing a 60-degree modified phase voltage and 5-switching angles.
   - **Switching Angles (Computed):** The computed switching angles are specified as 42.2759, 55.724, 62.807, 70.787, and 79.318 degrees.

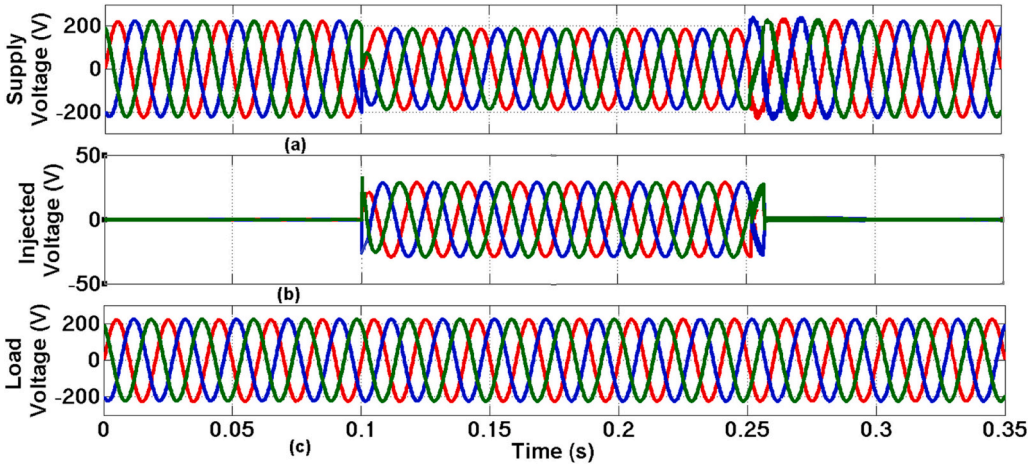

Fig. 8. Output voltage sag response of ZS-PV-FC based UPQC with R-L-C non-linear load (sensitive) and EV load when R-phase, Y-phase, B-phase and ground balanced fault for 5-switching (5th, 7th, 11th and 13th harmonic elimination) (a) Supply side voltage waveform for balanced 3-ϕ fault (b) by the proposed UPQC injected voltage (c) 3-phase non-linear load voltage waveform.

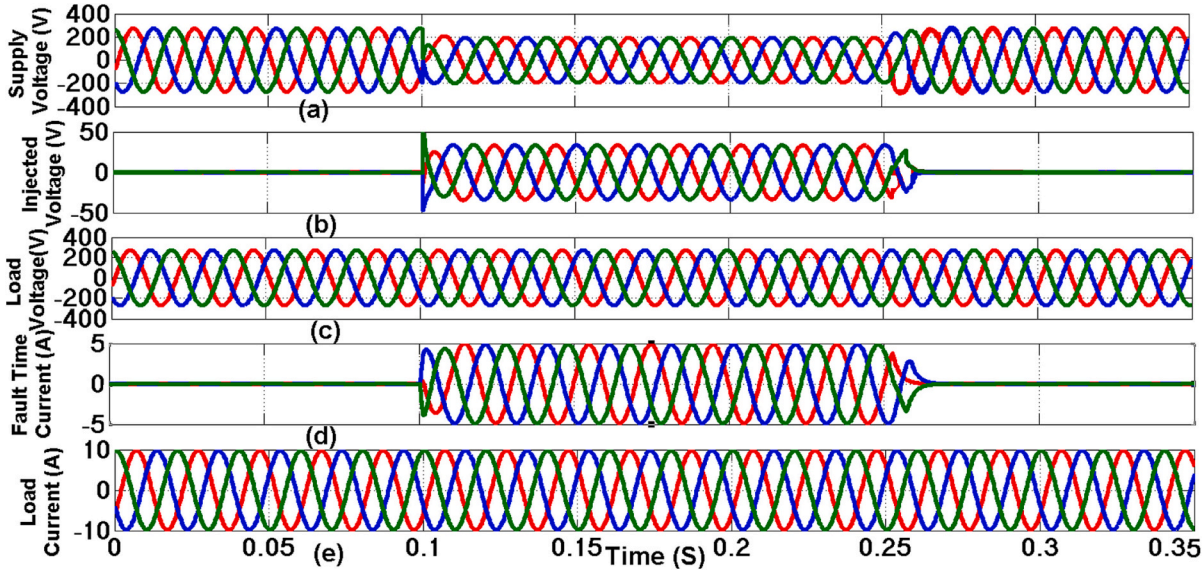

Fig. 9. Output voltage sag response of ZS-PV-FC based UPQC with R-L-C non-linear load (sensitive) and EV charging system when R-phase, Y-phase, B-phase and ground balanced fault for 7-switching (5th, 7th, 11th, 13th, 17th and 19 harmonic elimination) (a) Supply side voltage waveform for balanced 3-ϕ fault (b) by the proposed UPQC injected voltage (c) 3-phase linear load voltage waveform (d) 3-phase linear load current waveform for balanced fault (d) 3-phase balanced linear load current waveform.

iv. **Harmonic Analysis (% THD):**
- **Without Filter:** The total harmonic distortion (% THD) is calculated as 3.213 without the filter.
- **With Filter:** Introducing a filter result in a reduced % THD of 1.34.

v. **Harmonic Elimination (5-Switching):**
- **Harmonics Removed:** With the 5-switching strategy, the 5th order, 7th order, 11th order, and 13th order harmonics are effectively eliminated.

The simulation results showcase the robustness of the proposed FC-PV-Battery-Z source and BBO-based UPQC system in handling both balanced and unbalanced voltage swells. The detailed waveform analysis and harmonic elimination strategies demonstrate the system's capability to maintain stable load voltage while efficiently mitigating disturbances caused by voltage swells. The optimization achieved through modulation index adjustment and the application of switching angles contributes to the overall effectiveness of the proposed system.

Case study 5:

The supply side's three-phase unbalanced voltage waveforms are shown in Fig. 11. The presence of a swell between t = 0.1 and t = 0.25 s is demonstrated. The swell is 101 V, 82 V, and 41 V for A-phase, B-phase, and C-phase, respectively. The suggested UPQC system regulates the uneven swell voltage. The suggested UPQC system is also maintaining the load voltage depicted in Fig. 11(c).

The modulation index is then adjusted to 1, and the 120-degree conduction mode for 60-degree modified phase voltage with 5-switching angles. Computed switching angles are 42.1933, 55.7315, 62.5219,

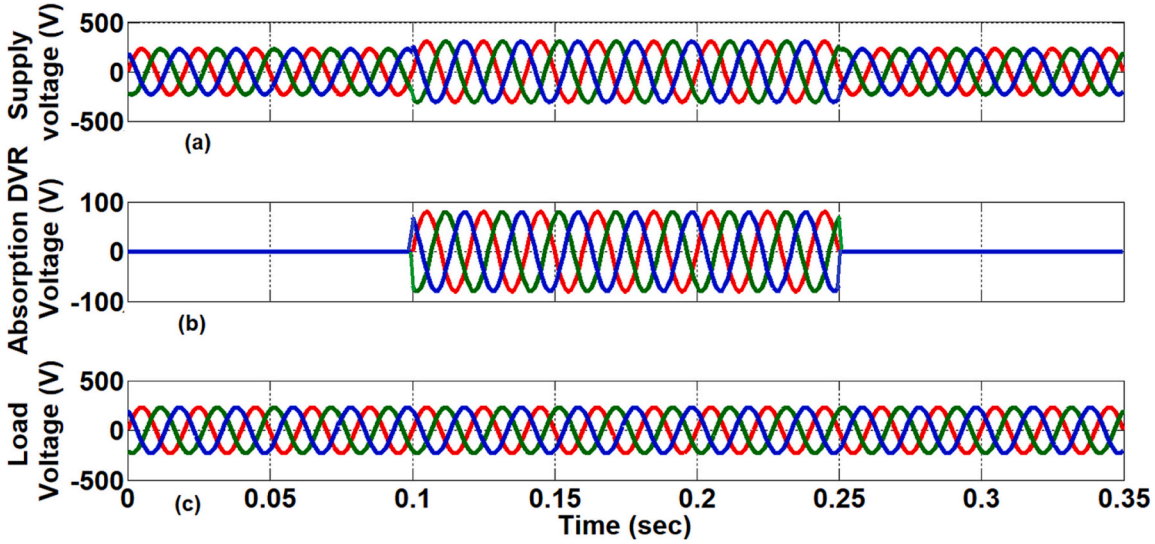

Fig. 10. Output voltage swells response of ZS-PV-FC based UPQC with capacitive non-linear load (sensitive) and EV system when R-phase, Y-phase, B-phase and ground balanced fault for 5-switching (5th, 7th, 11th and 13th harmonic elimination) (a) Supply side voltage waveform for balanced 3-ϕ fault (b) by the proposed ZS-FC-PV-UPQC balanced negative-injected voltage (c) 3-phase nonlinear load voltage waveform.

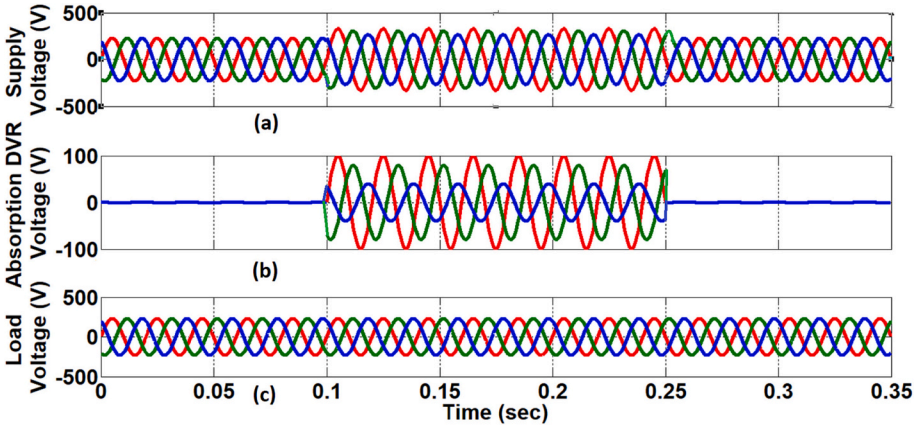

Fig. 11. Output voltage swells response of ZS-PV-FC based UPQC with capacitive nonlinear (sensitive) load and EV load when unbalanced fault for 5-switching (5th, 7th, 11th and 13th harmonic elimination) (a) Supply side voltage waveform for unbalanced 3-ϕ fault (b) by the proposed ZS-FC-PV-UPQC unbalanced negative-injected voltage (c) 3-phase nonlinear load voltage waveform.

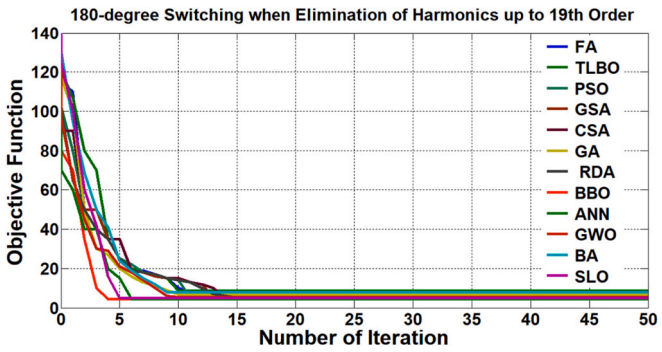

Fig. 12. The goal value with iterations for FA, TLBO, PSO, GSA, CSA, GA, RDA, BBO, ANN, GWO, BA and SLO method when $M_d = 0.91$ with elimination of harmonics up to 19th order.

70.6308 and 78.9052-degrees and the % THD is 3.031 by without filter but with filter the % THD is 0.97. For 5-switching, the 5th order, 7th order, 11th order and 13th order harmonics are eliminated.

Case study 6:

Fig. 12 illustrates the plot of the objective function versus the number of iterations for various optimization algorithms, including Firefly Algorithm (FA), Teaching-Learning-Based Optimization (TLBO), Particle Swarm Optimization (PSO), Gravitational Search Algorithm (GSA), Cuckoo Search Algorithm (CSA), Genetic Algorithms (GA), Red Deer Algorithm (RDA), Biogeography-based Optimization (BBO), Artificial Neural Networks (ANN), Grey Wolf Optimizer (GWO), Bat Algorithms (BA), and Soccer League Optimization (SLO) method, with a modulation index $M_d = 0.91$. Notably, BBO algorithm demonstrates the minimum number of iterations compared to other techniques after eliminating 5th to 19th order harmonics. The %THD levels and CPU time also exhibit minimum values for BBO technique, as detailed in Table 3. The comparative results in Table 3 affirm that among various Population-Based Optimization techniques, BBO algorithm stands out as a superior optimization method.

The effect of parameters on population-based optimization techniques for inverter harmonic elimination is a very importance. Population-based optimization techniques, such as FA, TLBO, PSO, GSA, CSA, GA, RDA, BBO, ANN, GWO, BA or SLO, are often used to find optimal solutions in complex and nonlinear optimization problems. In the context of inverter harmonic elimination, the goal is likely to minimize harmonic distortions in the output waveform of the inverter and improved the quality of power.

This study delves into the impact of varying the free parameters of BBO on the calculation of switching angles. Notably, it's evident that the population size plays a pivotal role in determining the accuracy of the computed angles. Other parameters, such as elitism parameters, mutation, and migration, exhibit minimal influence on the precision of the calculated angles. Tables 1, 2, and 3 showcase the calculated switching angles alongside voltage THD in %, considering same population sizes. The process indicates that optimizing performance falters when the population size is either too small or too large. A population size exceeding 50 satisfies suitability index variable (SIV) and habitat suitability index (HIS) but at the expense of BBO slowing down, taking longer to converge.

The parameters in these optimization techniques, such as crossover rates, mutation rates, population size, and convergence criteria, can significantly influence the performance of the optimization process. Adjusting these parameters can impact the speed of convergence, the quality of the solution found, and the ability of the algorithm to escape local optima. In Table 4 *shows the* Different Population- Based Optimization parameter.

5. Conclusion

This paper proposes a compensation control strategy for a comprehensive power conditioning system, the FC-PV-Battery-Z source-BBO integrated UPQC, designed for EV charging stations. This system combines fuel cells, photovoltaics, batteries, Z source network, and bidirectional boost converters to ensure high-quality power supply. The integrated UPQC actively addresses power quality issues, including voltage fluctuations and harmonics, providing a stable and efficient power source for sensitive loads and EV charging stations. This

Table 3
Optimization results for the different population-based optimization technique.

	FA	TLBO	PSO	GSA	CSA	GA	RDA	BBO	ANN	GWO	BA	SLO
Iteration	10	6	13	15	16	12	17	5	7	9	9	6
CPU time	0.6895	0.5806	0.6189	0.5253	0.4253	0.7363	0.6838	0.4132	0.5895	0.4899	0.4963	0.4235
%THD	7.645	8.785	4.987	4.936	4.563	6.713	5.242	4.496	4.5	5.427	6.878	4.821

Table 4
Parameter of different population-based optimization technique.

BBO		**GSA**	
Total population size	50	Number of agents	50
Generation count limit	50	Maximum number of iterations	50
Number of genes in each population member	5	Elitist Check	1 or 0
Mutation probability	0	Index of the test function	1
Habitat modification probability	1	Rpower	1
Initial mutation probability	0.005	Minimum flag	1
Elitism parameter	2	**GA**	
Lower bound for immigration probability per gene	0	Total population size	50
Upper bound for immigration probability per gene	1	Generation count limit	50
Step size used for numerical probabilities	1	Crossover type single point	1
Maximum immigration rate for each island	1	Crossover probability	1
Maximum emigration rate, for each island	1	Initial mutation probability	0.01
PSO		Elitism parameter	2
Elitism parameter	2	**CSA**	
Size of particle swarm neighbourhood	0	Number of iterations	50
Inertial constant	0.3	Discovery rate of alien eggs	0.25
Cognitive constant	1	Tolerance	1.00E-05
Social constant for swarm interaction	1	Lower bounds & Upper bounds	conditionally
Social constant for neighbourhood interaction	1	GWO	
Personal best of each particle	Population	Number of search agents	30
Neighbourhood best of each particle	Population	Maximum number of iterations	50
Global best	Population	lb is the lower bound:	−100
SLA		up is the upper bound	100
Lower Bound of Variables	−10	Set dimension	25
Upper Bound of Variables	10	TLBO	
Number of Decision Variables	200	Number of Unknown Variables	10
Number of Iterations	50	Unknown Variables Lower Bound	−10
Mutation Probability	0.1	Unknown Variables Upper Bound	10
Mutation Rate	0.2	Maximum Number of Iterations	50
Number of Teams	5	Population Size	50
Number of Main players	200	ANN	
Number of Reserve players	200	Number of Iterations	50
FA		Population size	50
Randomness 0–1 (highly random) alpha	0.5	RDA	
Minimum value of beta (betamn)	0.2	Number of Iterations	50
Absorption coefficient gamma	1	Population size	50
Number of iterations	50	Number of males, alpha, beta, gamma	15, 0.6, 0.4, 0.7

advanced solution aims to enhance system efficiency, protect equipment, and minimize power quality disturbances in the electrical network. Fuel Cell (FC) provide a reliable and continuous power supply to the system. Photovoltaic (PV) serves as a renewable power source, harnessing solar energy to complement the power generation from other sources. A battery system, typically based on lithium-ion technology, provides energy storage capability to the integrated system. It helps smooth out power fluctuations, store excess energy, and provide backup power during periods of low power generation or high demand. The Z source network is a power conversion topology that allows for voltage boosting and bucking operations while maintaining galvanic isolation. It enhances the flexibility and efficiency of power transfer between different components of the integrated system. Bidirectional Boost Converter is a power electronic converter that enables bidirectional power flow between the Z source network and the sensitive load or EV charging station.

The integrated UPQC functionality includes power factor correction, voltage regulation, harmonic mitigation, low % THD, and load balancing. It actively monitors and corrects power quality issues such as voltage sags, swells, harmonics, reactive power and unbalance to ensure a stable and high-quality power supply to sensitive loads and EV charging stations. This helps in protecting the equipment, enhancing system efficiency, and reducing power quality disturbances in the electrical network.

6. Future work

The proposed FC-PV-Battery-Z source-BBO integrated Unified Power Quality Conditioner (UPQC) system is a robust solution for addressing power quality issues in sensitive loads and EV charging stations. Here are a few promising directions for further research:

- **Advanced Control Algorithms:** Develop precise control algorithms, possibly integrating machine learning for adaptive optimization.
- **Energy Storage System Enhancement:** Research and implement advancements in energy storage systems, aiming for higher energy density, faster response times, and extended lifecycle. This could involve exploring emerging battery technologies or alternative energy storage solutions to improve overall system performance.
- **Adaptation for Emerging EV Technologies:** As electric vehicle technologies evolve, adapt the UPQC system to accommodate changes in EV charging infrastructure and standards. Consider developments in battery technologies, charging speeds, and vehicle-to-grid integration to ensure compatibility and optimal performance.
- **Dynamic Load Variation Studies:** Investigate system performance under varying loads, developing adaptable control strategies.
- **Hybrid Energy Management Strategies:** Optimize energy use from FC, PV, and the grid dynamically, considering weather, grid availability, and load demands.
- **Cyber-Physical Security Measures:** Implement robust cybersecurity to protect the system, especially in critical applications.
- **Scalability and Modularity:** Assess system adaptability for different scales of application, ensuring versatility.
- **Lifecycle Assessment and Environmental Impact:** Conduct a comprehensive environmental impact assessment for sustainability.
- **Field Implementation and Validation:** Validate system performance in real-world scenarios through field implementations.

- **Regulatory Compliance and Standards:** Ensure compliance with industry standards and regulations for reliability.
- **Cost Reduction Strategies:** Explore ways to reduce overall system costs, making the technology more accessible for widespread deployment.

By delving into these areas of future work, researchers and engineers can contribute to the advancement and practical applicability of the proposed system, fostering a more resilient and sustainable energy infrastructure.

CRediT authorship contribution statement

Krishna Sarker: Conceptualization, Methodology, Software, Validation, Formal analysis, Investigation, Writing – original draft, Writing – review & editing, Visualization.

Declaration of competing interest

The authors declare that they have no known competing financial interests or personal relationships that could have appeared to influence the work reported in this paper.

Data availability

The data that has been used is confidential.

References

[1] Muhammad Alif Mansor, Kamrul Hasan, Muhammad Murtadha Othman, Siti Zaliha Binti Mohammad Noor, Ismail Musirin, Construction and performance investigation of three-phase solar PV and battery energy storage system integrated UPQC, IEEE Access 8 (2020) 103511–103538. INSPEC Accession Number: 19660247, Electronic ISSN: 2169-3536, https://doi.org/10.1109/ACCESS.2020.2997056.

[2] N.C. Sai Sarita, S. Suresh Reddy, P. Sujatha, Control strategies for power quality enrichment in distribution network using UPQC, Mater. Today: Proc. 80 (3) (2023) 2872–2882, https://doi.org/10.1016/j.matpr.2021.07.053.

[3] Koganti Srilakshmi, Nakka Srinivas, Praveen Kumar Balachandran, Jonnala Ganesh Prasad Reddy, Sravanthy Gaddameedhi, Nagaraju Valluri, Shitharth Selvarajan, Design of soccer league optimization based hybrid controller for solar-battery integrated UPQC, IEEE Access 10 (October 3, 2022) 107116–107136, https://doi.org/10.1109/ACCESS.2022.3211504. NSPEC Accession Number: 22138510, Electronic ISSN: 2169-3536.

[4] Devi Prasad Acharya, Naeem Hannon, Subhashree Choudhury, Niranjan Nayak, Anshuman Satpathy, Design and hardware in loop testing of an intelligent controller for power quality improvement in a complex micro grid, Energy Rep. 9 (2023) 4135–4156, https://doi.org/10.2139/ssrn.4312781.

[5] Hamidreza Nazaripouya, Shahab Mehraeen, Modeling and nonlinear optimal control of weak/islanded grids using facts device in a game theoretic approach, IEEE Trans. Control Syst. Technol. 24 (1) (January 2016) 158–171. INSPEC Accession Number: 15683762, https://doi.org/10.1109/TCST.2015.2421434.

[6] Vinod Khadkikar, Enhancing electric power quality using UPQC: a comprehensive overview, IEEE Trans. Power Electron. 27 (5) (May 2012) 2284–2297. INSPEC Accession Number: 12571288, https://doi.org/10.1109/TPEL.2011.2172001.

[7] Santanu Kumar Dash, Pravat Kumar Ray, Power quality improvement utilizing PV fed unified power quality conditioner based on UV-PI and PR-R controller, CPSS Trans. Power Electron. Appl. 3 (3) (September 2018) 243–253. INSPEC Accession Number: 18229534, 10.24295/CPSSTPEA.2018.00024.

[8] Vinod Khadkikar, Ambrish Chandra, UPQC-S: a novel concept of simultaneous voltage sag/swell and load reactive power compensations utilizing series inverter of UPQC, IEEE Trans. Power Electron. 26 (9) (September 2011) 2414–2425. INSPEC Accession Number: 12241537, https://doi.org/10.1109/TPEL.2011.2106222.

[9] Han Jian, Li Xing, Yan Jiang, Shaonan Gong, Three-phase UPQC topology based on quadruple-active-bridge. Digital object identifier 10.1109/ACCESS.2020.3047961, IEEE Access 9 (December 30, 2020) 4049–4058. INSPEC Accession Number: 20322939, https://doi.org/10.1109/ACCESS.2020.3047961.

[10] Sisir Kumar Yadav, Ashish Patel, Hitesh Datt Mathur, Study on comparison of power losses between UPQC and UPQC-DG, IEEE Trans. Ind. Appl. 58 (6) (November/December 2022) 7384–7395. INSPEC Accession Number: 22292946, https://doi.org/10.1109/TIA.2022.3191985.

[11] Wu Dan, Fen Tang, Tomislav Dragicevic, Juan C. Vasquez, Member, and Josep M. Guerrero., A control architecture to coordinate renewable energy sources and energy storage systems in islanded microgrids, IEEE Trans. Smart Grid 6 (3) (May 2015) 1156–1166. INSPEC Accession Number: 15057498, https://doi.org/10.1109/TSG.2014.2377018.

[12] C.K. Sundarabalan, K. Selvi, PEM fuel cell supported distribution static compensator for power quality enhancement in three-phase four-wire distribution system, Int. J. Hydrog. Energy 39 (33) (November 11, 2014) 19051–19066, https://doi.org/10.1016/j.ijhydene.2014.09.086.

[13] Ali Reza Reisi, Mohammad H. Moradi, Hemen Showkati, Combined photovoltaic and unified power quality controller to improve power quality, Sol. Energy 88 (2013) 154–162, https://doi.org/10.1016/j.solener.2012.11.024.

[14] Ashish Patel, Sisir Kumar Yadav, Hitesh Datt Mathur, Utilizing UPQC-DG to export reactive power to grid with power angle control method, Electr. Power Syst. Res. 209 (August 2022), https://doi.org/10.1016/j.epsr.2022.107944.

[15] Sachin Tiwari, Seema Kewat, Bhim Singh, UPQC controlled solar PV-hydro battery microgrid, in: 2020 IEEE International Conference on Power Electronics, Drives and Energy Systems (PEDES), December 16–19, 2020, https://doi.org/10.1109/PEDES49360.2020.9379764. INSPEC Accession Number: 20510915.

[16] Mohammad Mohammadi, Javad S. Moghani, Jafar Milimonfared, A novel dual switching frequency modulation for Z-source and quasi-Z-source inverters, IEEE Trans. Ind. Electron. 65 (6) (June 2018) 5167–5176. INSPEC Accession Number: 17578097, https://doi.org/10.1109/TIE.2017.2784346.

[17] Dan Simon, Biogeography-based optimization, IEEE Trans. Evol. Comput. 12 (6) (December 2008) 702–713. INSPEC Accession Number: 1032452 6, https://doi.org/10.1109/TEVC.2008.919004.

[18] Krishna Sarker, Debashis Chatterjee, Swapan K. Goswami, Modified harmonic minimisation technique for doubly fed induction generators with solar-wind hybrid system using biogeography-based optimisation, IET Power Electron. 11 (10) (8/2018) 1640–1651, https://doi.org/10.1049/iet-pel.2017.0818.

[19] Vítor Monteiro, Carlos Moreira, Joao Abel Pecas Lopes, Carlos Henggeler Antunes, Gerardo J. Osório, João P.S. Catalão, João L. Afonso, A novel three-phase multiobjective unified power quality conditioner, IEEE Trans. Ind. Electron. 71 (1) (January 2024) 59–70, https://doi.org/10.1109/TIE.2023.3241380.

[20] Chandrakala Devi Sanjenbam, Bhim Singh, Modified adaptive filter based UPQC for battery supported hydro driven PMSG system, IEEE Trans. Ind. Inform. 19 (7) (July 2023), https://doi.org/10.1109/TII.2022.3215950.

[21] Chandrakala Devi Sanjenbam, Bhim Singh, Priyank Shah, Reduced voltage sensors based UPQC tied solar PV system enabling power quality improvement, IEEE Trans. Energy Convers. 38 (1) (March 2023) 392–403, https://doi.org/10.1109/TEC.2022.3197408.

[22] Anisha Heenkenda, Ahmed Elsanabary, Mehdi Seyedmahmoudian, Saad Mekhilef, Alex Stojcevski, Nur Fadilah Ab Aziz, Unified power quality conditioners based different structural arrangements: a comprehensive review, IEEE Access 11 (2023) 43435–43457. Electronic ISSN: 2169–3536 INSPEC Accession Number: 23117135, Publisher: IEEE, https://doi.org/10.1109/ACCESS.2023.3269855.

[23] Doğan Çelik, Hafiz Ahmed, Enhanced control of superconducting magnetic energy storage integrated UPQC for power quality improvement in EV charging station, J. Energy Storage 62 (June 2023), 106843, https://doi.org/10.1016/j.est.2023.106843.

[24] Ehsan Akbari, Abbas Zare Ghaleh Seyyedi, Power quality enhancement of distribution grid using a photovoltaic based hybrid active power filter with three level converter, Energy Rep. 9 (December 2023) 5432–5448, https://doi.org/10.1016/j.egyr.2023.04.368.

[25] Guilherme Masquetti Pelz, Sergio Augusto Oliveira da Silva, Distributed generation integrating a photovoltaic-based system with a single- to three-phase UPQC applied to rural or remote areas supplied by single-phase electrical power, Int. J. Electr. Power Energy Syst. 117 (May 2020), 105673, https://doi.org/10.1016/j.ijepes.2019.105673.

[26] A. Mousaei, M. Gheisarnejad, M.H. Khooban, Challenges and opportunities of FACTS devices interacting with electric vehicles in distribution networks: a technological review, J. Energy Storage 73 (A) (December 1, 2023), 108860, https://doi.org/10.1016/j.est.2023.108860.

[27] Joyal Isac Sankar, Srinath Subbaraman, Multi converter UPQC optimization for power quality improvement using beetle swarm-based butterfly optimization algorithm, Electr. Power Compon. Syst. 51 (20) (2023), https://doi.org/10.1080/15325008.2023.2210575.

[28] W. Li, W. Li, Y. Huang, Enhancing firefly algorithm with dual-population topology coevolution, Mathematics 10 (9) (2022) 1564, https://doi.org/10.3390/math10091564.

[29] Yu Kunjie, Xin Wang, Zhenlei Wang, An improved teaching-learning-based optimization algorithm for numerical and engineering optimization problems, J. Intell. Manuf. 27 (2016) 831–843, https://doi.org/10.1007/s10845-014-0918-3.

[30] S. Mirjalili, J. Song Dong, A. Lewis, A.S. Sadiq, Particle swarm optimization: theory, literature review, and application in airfoil design, in: S. Mirjalili, J. Song Dong, A. Lewis (Eds.), Nature-Inspired Optimizers. Studies in Computational Intelligence vol. 811, Springer International Publishing, Cham, Switzerland, 2020, pp. 167–184, https://doi.org/10.1007/978-3-030-12127-3_10.

[31] R. Shankar, N. Ganesh, R. Cep, R.C. Narayanan, S. Pal, K. Kalita, Hybridized particle swarm—gravitational search algorithm for process optimization, Processes 10 (3) (2022) 616, https://doi.org/10.3390/pr10030616.

[32] P. Kala, S. Arora, Implementation of hybrid GSA SHE technique in hybrid nine-level inverter topology, IEEE J. Emerg. Sel. Top. Power Electron. 9 (2021) 1064–1074.
[33] G.A.S. Joshi, O. Kulkarni, G.M. Kakandikar, V.M. Nandedkar, Cuckoo search optimization—a review, Mater. Today: Proc. 4 (8) (2017) 7262–7269, https://doi.org/10.1016/j.matpr.2017.07.055.
[34] S. Katoch, S.S. Chauhan, V. Kumar, A review on genetic algorithm: past, present, and future, Multimed. Tools Appl. 80 (2021) 8091–8126, https://doi.org/10.1007/s11042-020-10139-6.
[35] A.M. Fathollahi-Fard, M. Hajiaghaei-Keshteli, R. Tavakkoli-Moghaddam, Red deer algorithm (RDA): a new nature-inspired meta-heuristic, Soft. Comput. 24 (2020) 14637–14665, https://doi.org/10.1007/s00500-020-04812-z.
[36] M. Ali, M. Tariq, K.A. Lodi, R.K. Chakrobortty, M.J. Ryan, B. Alamri, C. Bharaetiraja, Robust ANN-based control of modified PUC-5 inverter for solar PV applications, IEEE Trans. Ind. Appl. 57 (2021) 3863–3876.
[37] S. Mirjalili, S.M. Mirjalili, A. Lewis, Grey Wolf optimizer, Adv. Eng. Softw. 69 (March 2014) 46–61, https://doi.org/10.1016/j.advengsoft.2013.12.007.
[38] Satılmıs Ürgün, Halil Yigit, Seyedali Mirjalili, Investigation of recent metaheuristics based selective harmonic elimination problem for different levels of multilevel inverters, Electronics 12 (2023) 1058, https://doi.org/10.3390/electronics12041058.
[39] M. Shehab, M.A. Abu-Hashem, M.K.Y. Shambour, A.Z. Alsalibi, O.A. Alomari, J.N. D. Gupta, A.R. Alsoud, L. Abuhaija, A comprehensive review of bat inspired algorithm: variants, applications, and hybridization, Arch. Comput. Methods Eng. 30 (2023) 765–797, https://doi.org/10.1007/s11831-022-09817-5.